UNIVERSIDADE FEDERAL DO CEARÁ
CÊNTRO DE CIÊNCIAS AGRÁRIAS
DEPARTAMENTO DE ENGENHARIA AGRÍCOLA
PROGRAMA DE PÓS-GRADUAÇÃO EM ENGENHARIA AGRÍCOLA

JULIANA ALCÂNTARA COSTA

WATER DYNAMICS IN THE SOIL-PLANT-ATMOSPHERE CONTINUUM IN SEMIARID FORESTS

FORTALEZA
2022

JULIANA ALCÂNTARA COSTA

WATER DYNAMICS IN THE SOIL-PLANT-ATMOSPHERE CONTINUUM IN SEMIARID FORESTS

Tese apresentada ao Programa de Pós-Graduação em Engenharia Agrícola da Universidade Federal do Ceará, como requisito parcial à obtenção do título de Doutor em Engenharia Agrícola. Área de concentração: Manejo e Conservação de Bacias Hidrográficas no Seminárido.
Orientador: Carlos Alexandre Gomes Costa
Coorientador: Lucas Melo Vellame
Coorientador estágio sanduíche: Joaquín Navarro-Hevia

FORTALEZA
2022

Dados Internacionais de Catalogação na Publicação
Universidade Federal do Ceará
Sistema de Bibliotecas
Gerada automaticamente pelo módulo Catalog, mediante os dados fornecidos pelo(a) autor(a)

C873w Costa, Juliana Alcântara.
Water dynamics in the soil-plant-atmosphere continuum in semiarid forests / Juliana Alcântara Costa. – 2022.
85 f. : il. color.

Tese (doutorado) – Universidade Federal do Ceará, Centro de Ciências Agrárias, Programa de Pós-Graduação em Engenharia Agrícola, Fortaleza, 2022.
Orientação: Prof. Dr. Carlos Alexandre Gomes Costa.
Coorientação: Prof. Dr. Lucas Melo Vellame.

1. ecohydrology. 2. Caatinga. 3. Pinares. 4. sap flow. 5. remote sensing. I. Título.

CDD 630

JULIANA ALCÂNTARA COSTA

WATER DYNAMICS IN THE SOIL-PLANT-ATMOSPHERE CONTINUUM IN SEMIARID FORESTS

Tese apresentada ao Programa de Pós-Graduação em Engenharia Agrícola da Universidade Federal do Ceará, como requisito parcial à obtenção do título de Doutor em Engenharia Agrícola. Área de concentração: Manejo e Conservação de Bacias Hidrográficas no Seminárido.
Orientador: Carlos Alexandre Gomes Costa
Coorientador: Lucas Melo Vellame
Coorientador estágio sanduíche: Joaquín Navarro-Hevia

Aprovada em: 09/09/2022.

BANCA EXAMINADORA

_____

Prof. Dr. Carlos Alexandre gomes Costa (Orientador)
Universidade Federal do Ceará (UFC)

_____

Prof. Dr. Lucas Melo Vellame (Coorientador)
Universidade Federal do Recôncavo da Bahia (UFRB)

_____

Prof. Dr. Joaquín Navarro Hevia (Orientador doutorado-sanduiche)
Universidad de Valladolid (UVa)

_____

Prof. Dr. José Carlos de Araújo
Universidade Federal do Ceará (UFC)

_____

Prof. Dr. José Vidal de Figueiredo
Instituto Federal de Educação, Ciência e Tecnologia do Ceará (IFCE)

_____

Prof. Dr. Everton Alves Rodrigues Pinheiro
Universidade Federal do Tocantis (UFT)

ACKNOWLEDGEMENTS

There would be no dissertation and much less I would be a doctor if it weren't for my dear advisors, Carlos Alexandre, Lucas Vellame, Joaquín Navarro and Zé Carlos. Yes, I was lucky to have 4 advisors, 4 tutors, 4 friends. Thank you for all the teaching shared and for keeping me motivated throughout the process.

I thank this educational institution that welcomed me since graduation.

To those who build the Graduate Program in Agricultural Engineering, who with competence and professionalism gave me the opportunity to do this.

To the colleagues of the Hidrosed group and of the Agricultural Engineering Department, Suzi, Italo, Thales, Gláuber, Aloys, Adão, Vidal, Arianna, Mácio Regys, Alisson Simplício, Christine for their collaboration throughout the process. I appreciate the good socializing, the good discussions, the good coffees and especially the help in setting up and conducting the experiment.

To the support of the University of Valladolid and to everyone who welcomed me during my time in Spain. To my colleagues at the University, to Professor Joaquín and his family, and to Ms. Carmen.

To Dona Socorro and Hosana Oliveira, who always welcomed us in Aiuaba.

To CAPES for granting the scholarship in Brazil and during the sandwich doctorate under the PRINT program (notice nº 41/2017).

To the WaR-Caatinga project (431639/2016-7) financed by CNPq, which guaranteed the purchase of material to manufacture the equipment used in the field experiment.

I also thank the meteorological agencies AEMET, INMET and FUCEME for the data provided for the present work.

To my family, for their love, encouragement and absolute support throughout the process.

To the person who has encouraged me the most in this final stretch, Lucas Roque.

And finally, to the psychiatrist, because without her I wouldn't have been able to handle it.

ABSTRACT

The movement and storage of water in forests play an important role in the integrated planning, development and management of water resources. These processes are particularly relevant in semi-arid regions. This document is divided into three chapters organized in the format of scientific articles. The entire PhD dissertation is based on the study of ecohydrological phenomena that occur in the soil-plant-atmosphere continuum. The chapters follow a broad line of investigation, starting with a more detailed hydrological process in a smaller area and ending with an approach in larger areas. The first chapter (I) is the one that, of the three, goes deeper into the study of the processes that occur in the soil-plant-atmosphere continuum, dealing with the variation of water storage in the plant in *Caesalpinia pyramidalis* Tul. and its relation to external events. In this first study, the Caatinga was used as an area designation. It was observed that the emergence of leaves occurred with a stem moisture of 0.32 $m^3.m^{-3}$. Catingueira plants are able to absorb water below the potential commonly determined as permanent wilting point (-1.5 MPa). The volume of water stored in the plants represents 17% of the maximum volume observed in the reservoir that receives all the water drained from the hydrographic basin during the study period. In the second chapter (II) it was intended to deepen the study of one of the phenomena related to evapotranspiration, the sap flow in the plant. In addition, in the second chapter, the study area was expanded to Tropical Seasonally Dry Forest, studying in particular the species *Caesalpinia pyramidalis* Tul., popularly known as catingueira, which is a strong representative of the biome that gives it its name. It was identified that catingueira plants have the ability to perform inverse sap flow at night and predawn basically throughout the year. Higher sap flow was observed in the transition seasons due to atmospheric conditions and soil moisture. There was a superiority of 46% of the catingueira sap flow in the rainy season compared to the dry season. It was noticed that the nocturnal sap flow is more significant in the driest months, demonstrating another adaptive strategy of the species. The third and final chapter (III) is the one with the broadest spatial approach of the three. The study deals with the hydrological process of evapotranspiration, which was carried out for two distinct semi-arid zones, one in Brazil (Caatinga) and another in Spain (Pinares), using remote sensing. It was found that the annual amplitude of potential evapotranspiration (ET_0) is the same in both areas, but the values of the Caatinga are higher. The Caatinga forest presented greater spatial variation of real Evapotranspiration (ETa) than the Pinares forest, as well as a greater extension with less temporal stability of the ETa than the Pinares forest. Both the Caatinga forest and the Pinares forest showed significant positive trends in annual ET_0 and ETa. We estimate that the value of

ETa increases faster in Pinares than in the Brazilian Caatinga. Taking the Caatinga as a hydrological mirror, some consequences are expected for Pinares, such as significant changes in the water balance, increased vulnerability of biodiversity and reduced water availability in the soil and in reservoirs.

Keywords: ecohydrology; Caatinga; Pinares; sap flow; remote sensing; evapotranspiration

RESUMO

O movimento e armazenamento de água em florestas desempenha um papel importante no planejamento, desenvolvimento e gestão integrados de recursos hídricos. Esses processos são particularmente relevantes nas regiões semiáridas. O presente documento encontra-se dividido em três capítulos organizados no formato de artigos científicos. Toda a tese é baseada no estudo de fenômenos ecohidrológicos que ocorrem no continuum solo-planta-atmosfera. Os capítulos seguem uma linha de ampliação de investigação, começando com um processo hidrológico mais detalhado em uma menor área e findando com uma abordagem em áreas mais amplas. O primeiro capítulo (I) é o que, dos três, mais se aprofunda no estudo dos processos que ocorrem no continuum solo-planta-atmosfera, tratando da variação de armazenamento de água na planta em *Caesalpinia pyramidalis* Tul. e de sua relação com eventos externos. Nesse primeiro estudo utilizou-se como designação de área a Caatinga. Observou-se o surgimento das folhas ocorreu com umidade caulinar de 0,32 $m^3.m^{-3}$. As plantas de catingueira são capazes de absorver água abaixo do potencial comumente determinado como ponto de murcha permanente (-1.5 MPa). O volume de água armazenada nas plantas representa 17% do volume máximo observado no reservatório que recebe toda a água drenada da bacia hidrográfica, durante o período de estudo. Já no segundo capítulo (II) pretendeu-se aprofundar no estudo de um dos fenômenos relacionados com a evapotranspiração, o fluxo de seiva na planta. Além disso, no segundo capítulo ampliou-se a área de estudo para Floresta Tropical Sazonalmente Seca, estudando em particular a espécie *Caesalpinia pyramidalis* Tul., conhecida popularmente como catingueira, que é uma forte representante do bioma que lhe dá o nome. Identificou-se que as plantas de catingueira apresentam a capacidade de realizar fluxo inverso de seiva no período noturno e predawn basicamente durante todo o ano. Foi observado maior fluxo de seiva nas estações de transição devido as condições atmosféricas e de umidade no solo. Verificou-se uma superioridade de 46% do fluxo de seiva da catingueira no período chuvoso em relação ao período seco. Percebeu-se que o fluxo de seiva noturno é mais significativo nos meses mais secos, demonstrando mais uma estratégia adaptativa da espécie**.** O terceiro e último (III) capítulo é o de abordagem espacial mais ampla dos três. O estudo trata do processo hidrológico evapotranspiração, que foi realizado para duas zonas semiáridas distintas, uma no Brasil (Caatinga) e outra na Espanha (Pinares), utilizando sensoriamento remoto. Verificou-se que a amplitude anual da evapotranspiração potencial (ET_0) é a mesma nas duas áreas, porém os valores da Caatinga são maiores. A floresta de Caatinga apresentou maior variação espacial da Evapotranspiração real (ETa) que a floresta de Pinares, bem como uma maior extensão com

menor estabilidade temporal da ETa que a floresta de Pinares. Tanto a floresta de Caatinga quanto a floresta de Pinares apresentaram tendências positivas significativas em ET_0 e ETa anuais. Estimamos que o valor da ETa aumenta mais rapidamente em Pinares do que na Caatinga brasileira. Tomando a Caatinga como espelho hidrológico, algumas consequências são esperadas para Pinares, como alterações significativas no balanço hídrico, aumento da vulnerabilidade da biodiversidade e redução da disponibilidade hídrica no solo e nos reservatórios.

Palavras-chave: ecohidrologia; Caatinga; Pinares; fluxo de seiva; sensoriamento remoto; evapotranspiração

SUMMARY

1 INTRODUCTION

Despite the great scientific effort that has been made in recent years to understand the dynamics of water in the soil-plant-atmosphere continuum, many gaps in knowledge are still open, mainly with regard to these processes in semiarid forests. Through this dissertation we seek to remedy some of these gaps.

The study was based on the following fundamental questions: what is the quantitative importance of the water stored in Caatinga tree species? What are the boundary ranges of moisture in the stem that trigger the process of leaf emission and growth? Are Caatinga species capable of performing inverse sap flow and when does this occur? What is the spacial and temporal pattern of actual evapotranspiration in semiarid forests in different parts of the globe? What is the temporal trend of evapotranspiration in semiarid forests?

This PhD dissertation is divided into three chapters organized in the format of scientific papers. The chapters follow a broad line of investigation, starting with a more detailed hydrological process in a smaller area and ending with an approach in larger areas. The first chapter (I) is the one that, of the three, goes deeper into the study of the processes that occur in the soil-plant-atmosphere continuum, dealing with the variation of water storage in the plant in *Caesalpinia pyramidalis* Tul. and its relation to external events. In the second chapter (II) it was intended to deepen the study of one of the phenomena related to evapotranspiration, the sap flow in the plant. In addition, in the second chapter, the study area was expanded to Tropical Seasonally Dry Forest, studying in particular the species *Caesalpinia pyramidalis* Tul., popularly known as catingueira, which is a strong representative of the biome that gives it its name. The third and final chapter (III) is the one with the broadest spatial approach of the three. The study deals with the hydrological process of evapotranspiration, which was carried out for two distinct semi-arid zones, one in Brazil (Caatinga) and another in Spain (Pinares), using remote sensing.

Thus, the objective of the thesis was to evaluate the water dynamics in the soil-plant-atmosphere continuum in semi-arid forests. For that we use data from different sources: in situ measurements, secondary data and satellite data. We work with sensors developed by our research group, HIDROSED (Hydrosedimentological Research Group of the Semiarid Region, <www.hidrosed.ufc.br>), to understand how the water storage and movement process takes place in the plant. We used remote sensing images to understand the process of water loss by evapotranspiration in semiarid forests on two different continents and under different

meteorological conditions. In other words, we worked in different ways to clarify the questions that guided our research and the results are presented below.

2 WATER STORAGE OF A TYPICAL TREE SPECIES IN THE CAATINGA BIOME (*Caesalpinia pyramidalis* Tul.)

Abstract: Our understanding of the movement and storage of water in typical Caatinga plants is still limited and often disregarded in water balance calculations. This is why the objective of this work was to evaluate the water storage dynamic in typical trees of the Caatinga biome during the dry, rainy and transition period by gauging the water content levels that cause the onset of leaf emergence. In a preserved Caatinga forest, soil and stem water content of six trees of the representative species catingueira (*Caesalpinia pyramidalis Tul*.) were monitored with low-cost capacitive sensors. Leaf moisture, leaf area index, leaf and stem water volume, and sap flow density were measured. The emergence of leaves occurred with a stem moisture of 0.32 $m^3.m^{-3}$, and the leaf area index showed its maximum level with a stem moisture of 0.34 $m^3.m^{-3}$. Catingueira plants are able to absorb water below the soil water potential commonly determined as the permanent wilting point (-1.5 MPa). The volume of water stored in the plants represents 108% of the average volume stored in the Boqueirão reservoir during the study period.

Keywords: Seasonally Dry Tropical Forest, ecohydrology, catingueira, stem moisture, sap flow

2.1 Introduction

In several regions of the planet the monitoring of hydrological variables has been intensified so as to seek to understand several processes, especially the relationship of water dynamics in the soil-plant-atmosphere continuum (SPAC). In arid and semi-arid ecosystems, vegetation cover produces a wide range of: hydrological effects (WANG et al., 2012), impacting surface runoff (SANTOS et al., 2017; VÁSQUEZ-MÉNDEZ et al., 2009), evaporation (ZHAO et al., 2021), erosive processes (SIMPLÍCIO et al., 2021), among others. Yet the understanding with regard to movement and storage of water in plants and their response to environmental factors is still limited.

Water stored in plant tissues benefits the respective plant by improving the canopy moisture status in periods of water deficit, thus increasing carbon assimilation and growth (KÖCHER; HORNA; LEUSCHNER, 2013). It is, however, still unclear how certain ecohydrological characteristics influence plant survival during drought or how water storage in plants impacts their water balance, especially in semi-arid ecosystems such as the Caatinga biome, given all the unique hydrological processes that occur in this region, such as the deciduosity of leaves, specific physiological adaptations of vegetation and the seasonality of precipitation (DOMBROSKI et al., 2011).

Knowledge of water storage in plants helps to solve critical questions in forest research and to elaborate a system for the efficient use of water resources (LIANG et al., 2020), still, in most hydrological models and also the broader concept of water availability in the Caatinga the water contained in plants is disregarded. And due to the deciduous behaviour of the biome the importance of stem moisture as an inducing agent of leaf emission and senescence is not known. That is why the following two fundamental questions were elaborated and they will be addressed in this study: what is the quantitative importance of the water stored in Caatinga tree species compared to other water reservoirs? What are the boundary ranges of moisture in the stem that trigger the process of leaf emergence?

The method commonly used to obtain stem moisture is the gravimetric analysis, in which the variable is measured based on the difference in weight before and after oven drying (DAHLEN; SCHIMLECK; SCHILLING, 2020; LÓPEZ-BERNAL; TESTI; VILLALOBOS, 2012). According to Liang et al. (2020) this methodology has a significant disadvantage since it destroys the samples taken from the trunk of the tree studied. In this sense, water content sensors have lately been presented as a viable alternative (DAHLEN; SCHIMLECK; SCHILLING, 2020), as they are non-destructive and provide rapid response as well as the possibility of continuously monitoring the humidity in the same plant. This equipment consists

of sensors which function on the basis of resistive and capacitive principles (DONATO et al., 2014) and, when calibrated, present an excellent correlation with the gravimetric method (ARAÚJO et al., 2021).

Thus, the objective of this chapter was to evaluate the dynamics of soil moisture in the root zone and water storage in catingueira plants (*Caesalpinia pyramidalis Tul.*) during the three periods: dryness, rain and transition, and to assess the moisture levels that cause the leaf growth process.

2.2 Materials and Methods

2.2.1 Study area

This study was carried out in the Aiuaba Experimental Basin (AEB, 12 km²) located in the southwest sector of the Ecological Station (ESEC) of Aiuaba, which is fully composed of the Caatinga biome in an initial stage of secondary succession and inserted in the semi-arid region of northeastern Brazil (Figure 1). The Aiuaba ESEC was established in 1978, is associated with the maintenance of the flora and fauna biodiversity of the Caatinga biome and plays an important role in the region's hydrological cycle, mainly due to its dense forest cover (DE ARAÚJO; PIEDRA, 2009). According to the Köppen classification, the climate of the region is BSh (tropical semi-arid) with potential evapotranspiration of 1990 mm.year^{-1}, an average precipitation of 583 mm.year^{-1} and an average annual temperature of 25 ºC (COSTA et al., 2021). The basin has an artificial reservoir named Boqueirão with a maximum capacity of 0.06 hm³ at its outlet (DE ARAÚJO; PIEDRA, 2009).

Figure 1 - Location map of the study area in Aiuaba, Ceará, Brazil, including dispositions of monitored catingueira plants

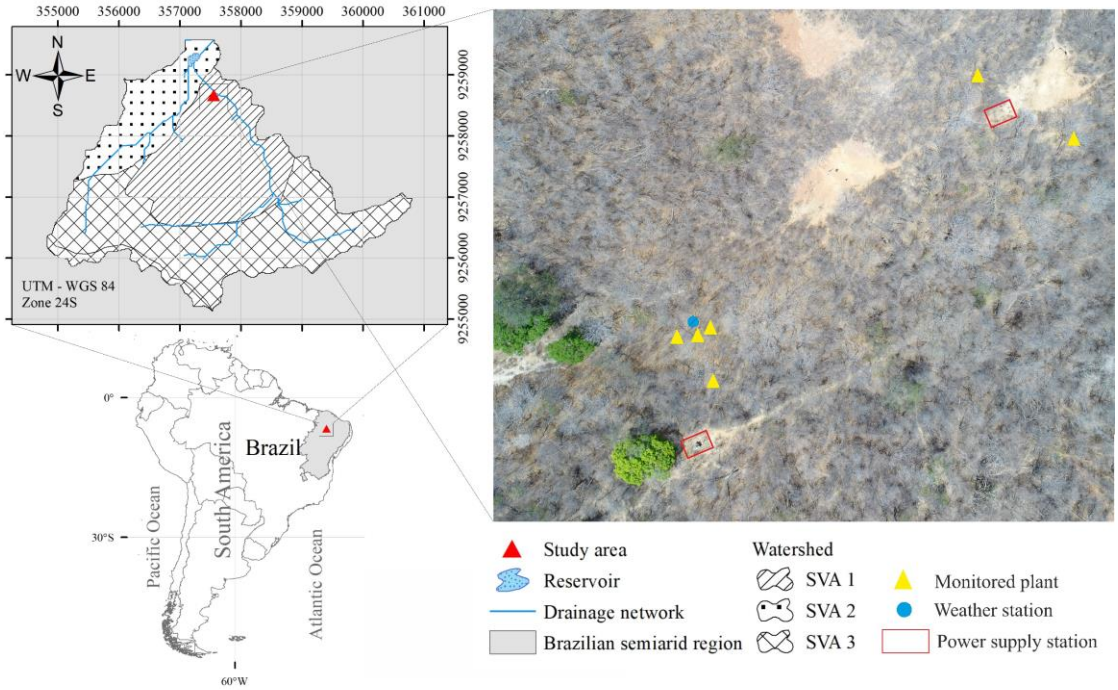

The Aiuaba Experimental Basin (AEB) has been monitored since January 2003 by the study group HIDROSED (Hydrosedimentological Research Group of the Semiarid Region, <www.hidrosed.ufc.br>). Studies carried out in the basin during this period include

measurements and analysis of hydrological variables, such as precipitation, evaporation, evapotranspiration, surface runoff and losses from plant interception (COSTA et al., 2021; DE ARAÚJO; PIEDRA, 2009; DE FIGUEIREDO et al., 2016; MEDEIROS; DE ARAÚJO; BRONSTERT, 2009) besides hydrogeological and sedimentological studies (COSTA et al., 2013, 2016; PINHEIRO et al., 2016; PINHEIRO; VAN LIER; METSELAAR, 2018), among others. The AEB is divided into three soil-vegetation associations (SVA). The first association (SVA1) occupies 20% of the area with Acrisol and the depth of the root zone of the plants is 80 cm. The second system (SVA2) can be found in 34% of the area, it presents soils classified as Luvisols and the average depth of the root zone is 60 cm. SVA3 takes up 46% of the basin area, has shallow soil (Regosol) and a rooting depth of 40 cm (COSTA et al., 2016; PINHEIRO et al., 2016).

Even with the high floristic diversity of the Caatinga, some species are considered representative of the biome, as they are the most abundant in certain SVAs (GÜNTNER; BRONSTERT, 2004). The study was carried out with six adult catingueira plants (*Caesalpinia pyramidalis Tul*.) located in SVA1 (Figure 1). This is the most representative tree species in the experimental area (table 1) and has potential for veterinarian and medicinal use, for reforestation and agroforestry and as fodder for sheep and cattle (LOPES et al., 2017). Its wood is used for posts and fences, in the construction of adobe houses, as firewood and for charcoal; due to its robustness, it is also suitable for reforestation.

Table 1 - Phytosociological parameters of Catingueira (*Caesalpinia pyramidalis Tul*.) sampled in the three soil-vegetation associations (SVA) of the Aiuaba Experimental Basin

Area	AD	RD	RDo	RF	CVI	IVI
SVA1	256.0	7.40	13.50	14.30	10.50	11.70
SVA2	0.0	0.00	0.00	0.00	0.00	0.00
SVA3	7.1	0.21	0.21	1.59	0.67	0.21

AD: Absolute Density (ind.ha^{-1}), RD: Relative Density (%), RDo: Relative Dominance (%), RF: Relative Frequency (%), CVI: Coverage Value Index and IVI: Importance Value Index.

2.2.2 Instrumentation for in situ monitoring

2.2.2.1 Soil and stem moisture measurement

Soil and stem moisture were monitored for a period of one year (11/05/2020 to 11/05/2021) in six plants using low-cost capacitive sensors (ARAÚJO et al., 2021). These have metal rods as electrodes, so variations in the dielectric constant and electrical resistance of the rod also change the frequency of an oscillator (integrated circuit 555) which is read by an

Arduino Pro-Mini board and transmitted via serial communication (Figure 2) (ARAÚJO et al., 2021).

Figure 2 - Electronic diagram of stem moisture sensors

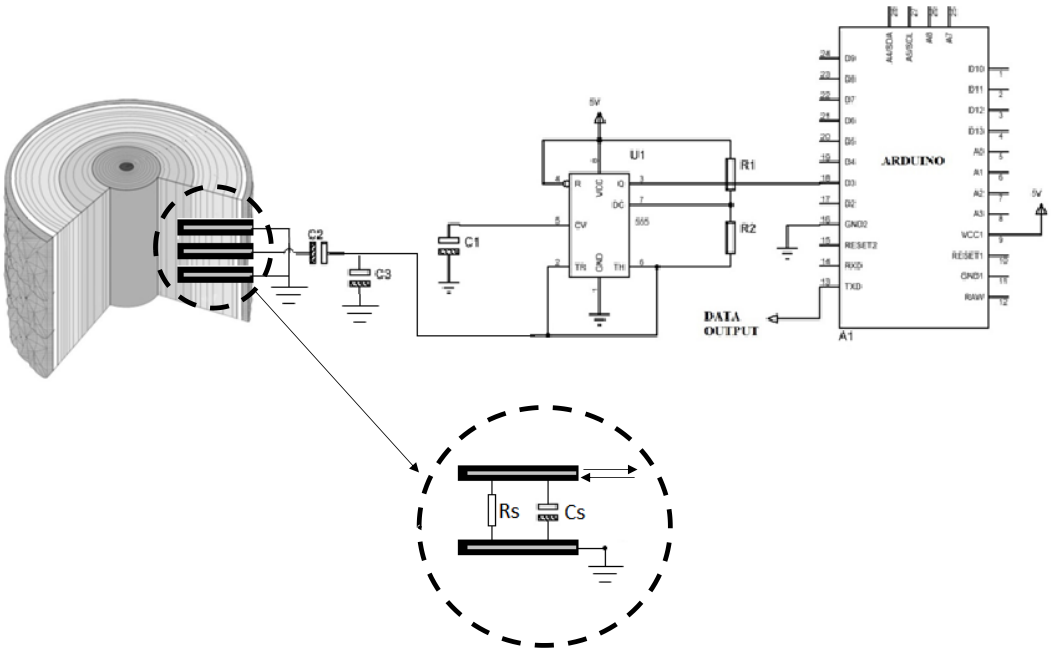

The sensors were calibrated using four soil samples (Figure 3a) and three stem samples (Figure 3b), taken from the study area (Figure 3). Three sensors were installed in each catingueira plant, two for soil moisture, at 0.2 m and 0.4 m depth (Figure 4a) in the root zone and a stem moisture sensor (Figure 4b). The equations that best fit the data were those shown in Figure 3. Data were collected and stored using data loggers built with an Arduino system at a frequency of 10 min.

Figure 3 – Calibration equation for soil (a) and stem (b) moisture sensors (MS)

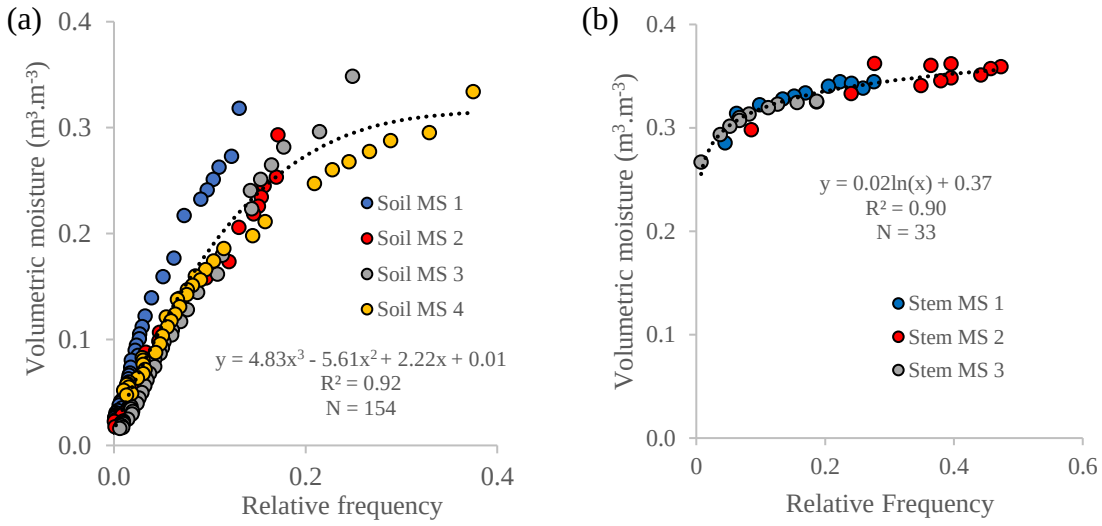

Figure 4 – Soil moisture sensors installed in the root zone of the plants at 20 cm and 40 cm depth (a) and moisture sensor installed in the stem of one of the catingueira plants (b)

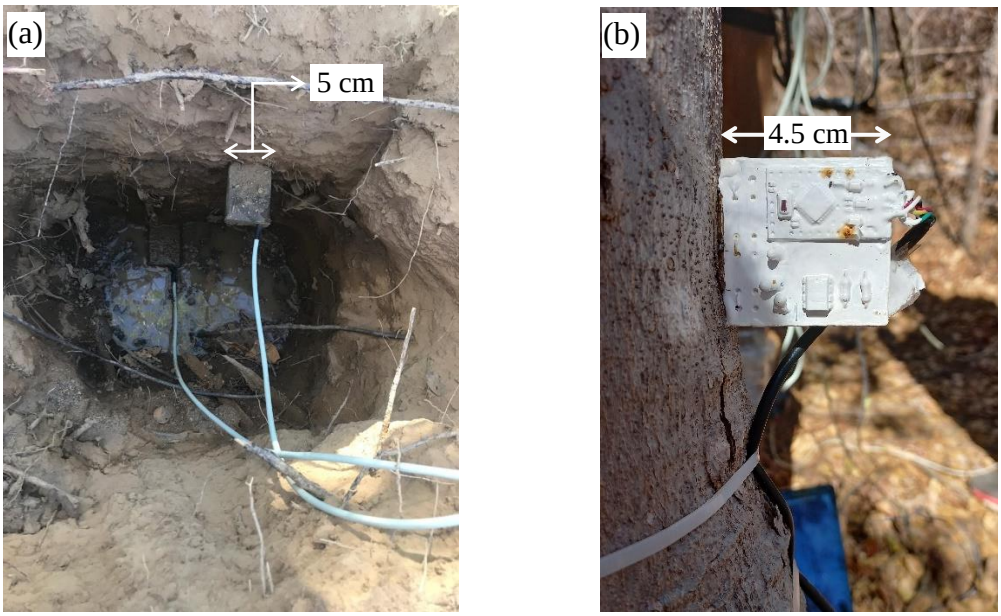

2.2.2.2 Meteorological data

Rainfall data were obtained at a rainfall station installed in the study area with a tipping rain gauge, and measurements were stored every 5 min in a Campbell scientific data logger from 11/05/2020 to 11/05/2021. Data on relative humidity, wind speed, air, soil and canopy temperatures as well as on global solar radiation were also obtained. These variables were provided by a low-cost automatic weather station installed in the study area, while measurements were stored at home for 10 min from 12/06/2020 to 05/10/2021.

2.2.2.3 Measurements of sap flow density in the stem

In the six plants used in the study, sensors were also installed to determine density and direction of the sap flow during the period from 11/05/2020 to 11/05/2021. The method used was the heat ratio method (HRM) developed by Burgess et al. (2001). It measures the temperature increase rate after the release of a heat pulse, at equidistant points downstream and upstream of a heating probe. The heat pulse velocity (cm h^{-1}) is calculated according to equation 1:

$$Vh = \frac{4kt\ ln\ ln\left(\frac{v_1}{v_2}\right) - x_2^2 + x_1^2}{2t(x_1 + x_2)}\beta 3600 \quad (1)$$

Where: k is the thermal diffusivity of fresh wood ($cm.h^{-1}$), x_1 and x_2 are the corrected distances (cm) between the heater and the temperature probe, and v_1 and v_2 are temperature increases (with respect to initial temperatures) at equidistant points downstream and upstream, respectively, and t is the measurement time (s).

The probe positions relative to the heater used with the HRM are –0.6 and 0.6 cm, so x = 0.6 cm. Thermal diffusivity (k) is given a nominal value of $2{,}5 \times 10^{-3}$ cm^2 s^{-1} (MARSHALL, 1958). Installing sensors in xylem tissue causes substantial mechanical damage. In addition to the interruption of flow paths by the insertion of probes, intact vessels can become occluded as the plant responds to injury by forming tyloses. The resulting region of non-conductive wood around the probe insertion site affects the Vh measurement by decreasing the v_1/v_2 ratio. To correct this error, we use the coefficient β admitted as 1.7023 by Burgess et al. (2001) for a probe insertion diameter of 0.17 cm.

Even if the probes are carefully placed, the spacing between them is likely to be at least somewhat asymmetrical. This is why probe positioning must be corrected by equation 2 (BURGESS et al., 2001):

$$x_2 = \sqrt{\left(4kt \ln\left(\frac{v_1}{v_2}\right) + x_1^2\right)} \quad (2)$$

Where: x2 denotes the incorrectly spaced probe, x1 is assumed to be correctly spaced at 0.6 cm and t is the measurement time.

Since it is not known which of the two probes is incorrectly positioned, equation 2 is solved by assuming that x1 is correctly positioned. Ratios between v1/v2 will asymptotically approach an ideal value and the rate of change will exponentially decay after the heat pulse.

Thus, (BURGESS et al., 2001) suggest that measurements be made 60 and 100s after heat pulse release, when v1/v2 is effectively linear.

Only a portion of the xylem tissue (the sapwood, hydroactive xylem) contains moving sap. Heat pulse probes effectively measure a weighted average of the velocities of moving sap and "stationary" wood. Sap velocity (also called sap flow density) can be determined by measuring the fractions of sap and wood in the xylem and considering their different densities and specific heat capacities according to equation 3.

$$V_s = \frac{Vc\rho_b(C_w + m_c C_s)}{\rho_s C_s} \quad (3)$$

Where: Vc is the corrected heat pulse velocity ($cm.h^{-1}$), ρ_b the basic wood density (dry weight/green volume, in $kg.cm^{-3}$). C_w and c_s are the specific heat capacity of wood matrix (1200 $J.kg^{-1}.°C^{-1}$) and sap (4182 $J.kg^{-1}.°C^{-1}$), respectively. M_c is the water content of sapwood and ρ_s is water density ($kg.cm^{-3}$).

2.2.3 Water volume in the leaves

Six leaf samples were evaluated in 4 data collection campaigns which took place during the rainy season (Jan-Apr) and the wet-dry transition period (May), a time when plants have leaves, since their foliage is deciduous. The samples were taken to the laboratory and weighed to obtain the fresh mass, later placed in an oven to dry for 24 hours. After obtaining the dry mass, the leaf water content (LWC) was calculated through the relationship (equation 4):

$$LWC = \frac{FM - DM}{DM} \quad (4)$$

Where: FM is the fresh mass of the sample (g) and DM is the dry mass of the sample (g).

The correlation equation LM = 41,315 StM - 12,666 with $R^2 = 0.56$ was obtained by relating the stem moisture data to leaf moisture (LM). Through this relationship, it was possible to estimate leaf moisture for the other days of the monitoring period and gather information about water storage in the canopy.

Since evapotranspiration is a surface phenomenon, it was assumed that the leaf area index (LAI) is linearly linked to the ratio between latent heat and net radiation (equation 5). The maximum LAI for catingueira was determined by Pinheiro et al. (2016) and has a value of 0.97.

$$LAI(t) = LAI_{max} \frac{(LE/Rn)(t)}{(LE/Rn)_{max}} \quad (5)$$

Where: LE is the latent heat of vaporization (mm), Rn is net solar radiation (mm), $LAI_{máx}$ is the maximum leaf area index ($m^2.m^{-2}$) and t is time.

The IAF was calculated whenever data from the automatic station were available for the period from 12/06/2020 to 05/10/2021. Equation 6 was used to calculate LE. Given that canopy temperature is a response to energy exchanges, the energy used for evapotranspiration can be determined based on the leaf energy balance (GATES, 1968) and the radiation balance in the canopy (Figure 5).

$$LE = (E - \alpha)\, Rg - 2\, \varepsilon\, \sigma\left(T_c^4 - \varepsilon\, T_a^4\right) - K_a \frac{T_c - T_a}{K_f \sqrt{\frac{w}{u}}} \quad (6)$$

Where: E is the solar radiation interception efficiency, α the surface albedo, Rg is the global radiation ($W.m^{-2}$), ε the ambient long wave emissivity (0.96), σ is the constant of Stefan-Boltzmann ($5.6704\ 10^{-8}\ W.m^{-2}.K^{-4}$), Tc is canopy temperature (K), Ta is air temperature (K), Ka is the convective-conductive conductivity of the air ($0{,}0259\ W.m.K^{-1}$), Kl is the empirical leaf shape parameter ($0{,}0057\ m.s^{-0,5}$), w the leaf width (m) and u is wind speed ($m.s^{-1}$).

Figure 5 - Radiation balance in crown and leaf indicates global shortwave radiation (Rg), radiation transmitted to the ground (Rt), reflected radiation (α.Rg) under the effect of the albedo (α) and interception efficiency (E)

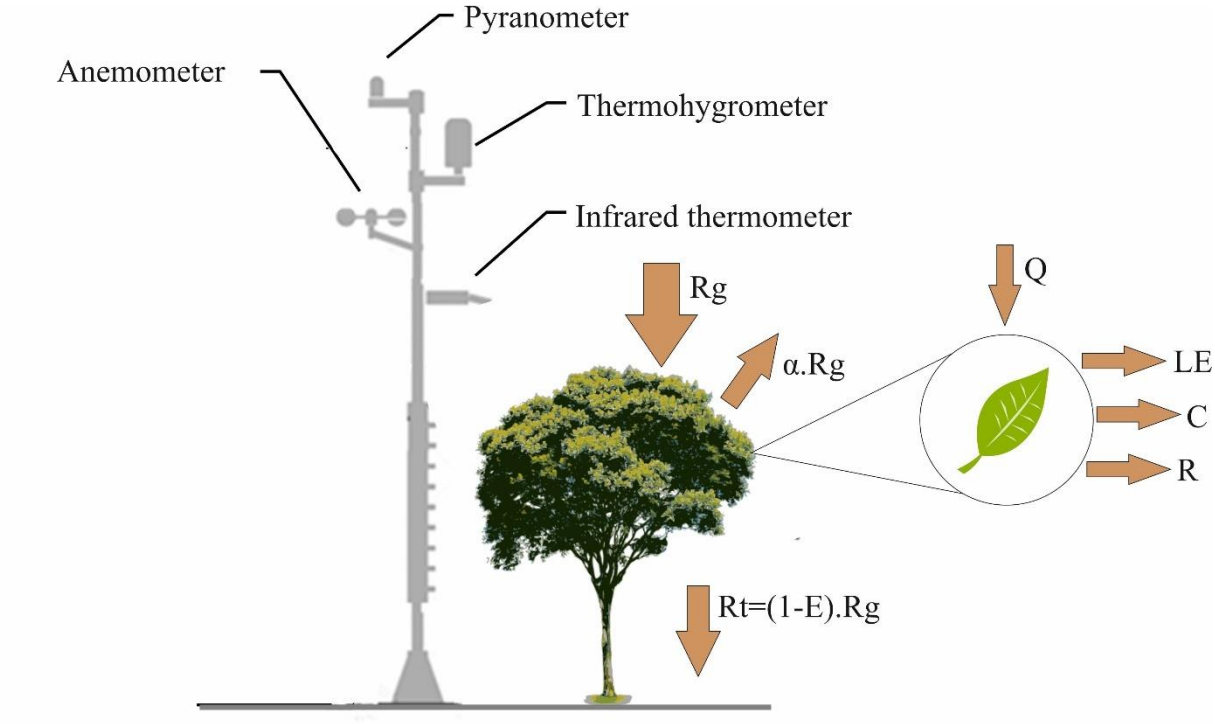

Equation 7 was used to calculate the volume of water stored in the leaves (LWS):

$$LWS = LM.LAI.area.LMA \quad (7)$$

Where: LM is moisture in the leaves ($g.g^{-1}$), LAI is the leaf area index ($m^2.m^{-2}$), area is the land surface (m^2) from which one wants to obtain the water stored in the leaves and LMA is leaf mass per area, calculated as the ratio between leaf dry mass (g) and leaf area (m^2).

2.2.4 Water storage in the plant

The volume of water stored in the stem (StWC) was estimated through the product of stem volume (m^3) and stem moisture ($m^3.m^{-3}$) data. Equation 8 (Schumacher and Hall, 1933 adaptada para a Caatinga por Alves Junior, 2010) was used to estimate the stem volume (Vst).

$$Vst = 0{,}021 CBH^{1{,}799} H^{1{,}361} \quad (8)$$

Where: CBH is the circumference at breast height (m) and H is the height of the plant (m). Equation 9 was employed for the estimation of aboveground tree water storage (PWS, m^3):

$$PWS = StWC + LWC \quad (9)$$

Where: StWC is the volume of water in the stem (m^3) and LWC is the volume of water in the leaves (m^3).

The plant water storage data in the study area were presented in millimeters (mm) through the relationship between PWS and the number of catingueira trees per square meter in each SVA.

2.3 Results and Discussion

Throughout the year soil moisture varies more than stem moisture, especially at the beginning of the rainy season significant increases can be observed (Figure 6). The reduction in stem moisture, on the other hand, occurs in stages after the rainy season, which indicates that plants are able to retain water in their tissues until the release of water is necessary and a new adjustment must be made.

Figure 6 – Daily average of water stored in the soil (0 - 56 cm) and in the catingueira stem, leaf area index and precipitation during the period from November 2020 to November 2021

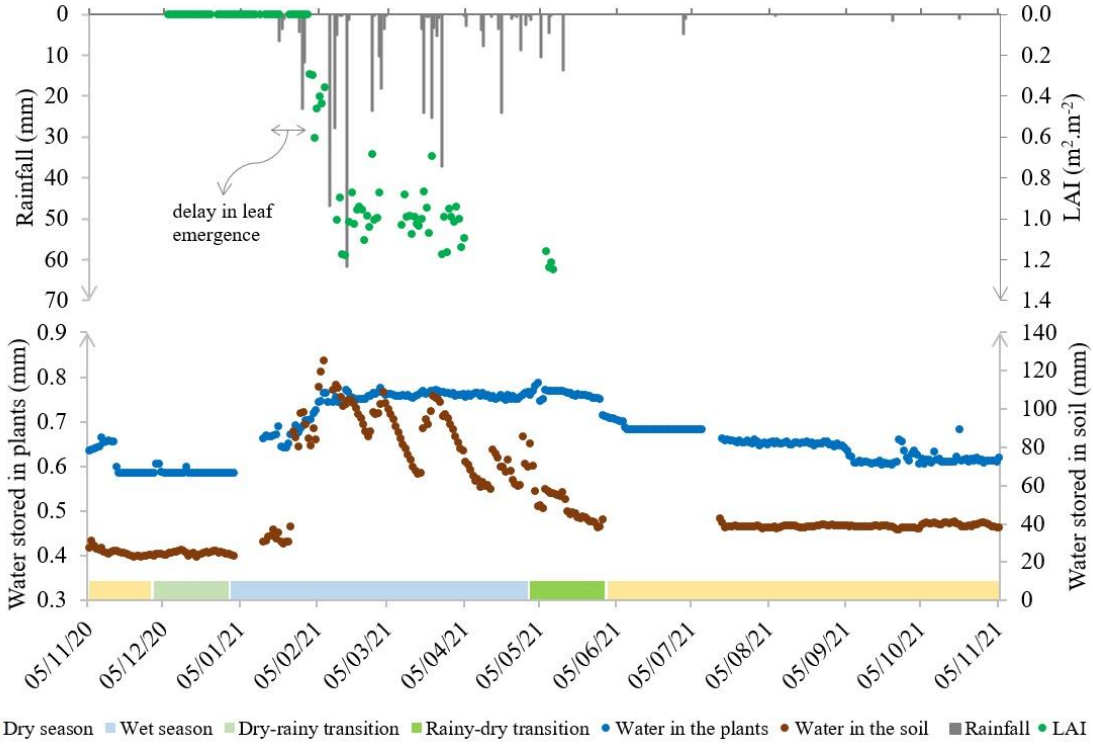

The physiological capacity developed by the plants of the Caatinga biome and their adaptive structures provide the water storage that contributes to the transpiration process, reduces competition for water with neighboring plants and guarantees water supply during periods of drought (HARTZELL; BARTLETT; PORPORATO, 2017). Water storage capacity increases with an increment in sapwood volume or with a decrease in wood density (BORCHERT, 1994; CARRASCO et al., 2014; HARTZELL; BARTLETT; PORPORATO, 2017; LIMA; RODAL, 2010). In seasonally dry tropical forests, species can be classified as: low wood density deciduous (*Amburana cearenses, Commiphora leptophloeos*), high wood density deciduous (*Caesalpinia pyramidalis, Croton blanchetianus*) or high wood density perennial species (*Cynophalla flexuosa , Ziziphus joazeiro*) (WRIGHT et al., 2021).

Wright et al. (2021) classify the catingueira among Caatinga species as deciduous with high wood density (0.64 g cm^{-3}). According to Borchert (1994) species with dense wood and low water storage capacity in the stem delay leaf fall until the dry season. At the time of leaf abscission, the water potentials of leaves and branches of these trees are quite negative (<-4 MPa, according to Borchert (1994)) and their stem water amount is substantially reduced in relation to the levels during the rainy season (decrease of 20%, as specified in the data compiled for this study). Species with low wood density, in contrast, are more sensitive to drought. These species are the first to lose their leaves at the onset of the dry season. Corroborating the thesis raised above, the catingueira is one of the last deciduous species of the Caatinga to lose its leaves during dry season. In the Aiuaba Experimental Basin, the catingueira presents leaf cover until mid-August, and some leaves in the lower third of the crown, in shadier locations, remain even until early October (DE ALMEIDA; DE CARVALHO; DE ARAÚJO, 2019). It may, therefore, be stated that high wood density, which results in a lower water content and more negative water potential, possibly is the cause of the gradual water storage reduction in the catingueira tree.

Hartzell et al. (2017) comment that the hydraulic characteristics of a plant vary in two aspects: drought tolerance and drought prevention. This means that plants with a drought-tolerant water use strategy tend to have a low hydraulic capacitance, higher wood density and greater tolerance regarding hydraulic stress. Plants with a drought-avoidance strategy, on the other hand, tend to have high hydraulic capacitance, low wood density and high vulnerability to cavitation at low water potentials. As wood density increases, plants typically become more tolerant of water stress.

While plants use mechanisms to maintain water in their structures, the soil in the root zone gets drier and drier (Figure 6), it loses moisture through root absorption and evaporation until its water potential is so low that water withdrawal is no longer observed unless water is recharged again. Understanding soil and plants as water reservoirs, it can be said that the soil, despite its retention characteristics and interactions with plants and organic matter, is a reservoir with less water use management, or with a water management strategy based on releasing water while it is available. Plant reservoirs, on the contrary, possess regulatory agents for water release.

In the rainy season the volume of water stored by the leaves corresponds to 1% of the total water stored by the plants, since most of the plant biomass is in the branches and stems, which manage to maintain relatively high water contents during that season. Yet, this

percentage of water stored in the leaves is likely to be disregarded in water storage calculations concerning catingueira plants.

The annual amplitude in plant water storage between the dry, rainy, dry-rainy and rainy-dry transition seasons is 0.20 mm. In the other evaluated compartment, the soil, the annual storage amplitude in the area of the catingueira roots is 80 mm. The volume of water stored in plants can, however, represent an important part of the water storage in a watershed, and in this work the average volume found per plant was 27 liters (average of 29 liters in the rainy season and 25 liters in the dry season). According to a phytosociological survey (table 1) the population density of catingueira individuals in SVA1 is 256 per hectare, representing around 7.0 m³ of water per hectare. It is noteworthy that this species only represents 10.5% of the vegetation cover in the area.

The water volume in catingueira plants is of great importance in the water balance of the basin: the amount stored in all the SVAs was 1729 m³ (table 2). The average water volume in the plants represents 108% of the average volume observed in the Boqueirão reservoir during the study period.

Table 2– Synthesis of water storage data in catingueira plants (*Caesalpinia pyramidalis Tul.*) and comparison with the volume stored in the Boqueirão reservoir

Variables	Values
circumference at chest height (m)	0.42 ± 0.12
plant height (m)	6.81 ± 0.79
average plant volume (m^3)	0.09 ± 0.05
volume of water stored in catingueira plants:	
for each plant (m^3)	0.026 ± 0.003
All catingueira trees in SVA1 (m^3)	1625
All catingueira trees in SVA2 (m^3)	0
All catingueira trees in SVA3 (m^3)	104
All catingueira trees in AEB (m^3)	1729
Relationship between the maximum volume of water stored in catingueira in the experimental basin AEB and the maximum volume stored in the Boqueirão reservoir during the study period (11885 m^3) (%)	17
Relationship between the average volume of water stored in catingueira in the AEB and the average volume stored in Boqueirão during the study period (1601 m^3) (%)	108
Relationship between the minimum volume of water stored in catingueira in the AEB and the average volume stored in Boqueirão during the study period (1000 m^3) (%)	141

Tilesse et al. (2021) analyzed the potential water storage capacity in catingueira wood and quantified a 3% relationship between the volume stored in the plants and the

maximum capacity of Boqueirão (0.06 hm3). Most hydrological models, such as the SWAP (KROES et al., 2009), consider that all water absorbed from the soil by plants is used on a daily basis for transpiration. Possibly, the disregard of data related to water storage in the plant is one of the reasons for errors found in the application of such models in the semiarid region. Pinheiro et al. (2016), used SWAP in the Aiuaba Experimental Basin and found prediction errors of 4.3%.

New leaves emerge on a plant after water is replenished by the root and stem biomass; there is, however, a delay of approximately 10 days between the LAI increase and the moment when soil and stem moisture rise (Figure 6). This period between the beginning of the rainy season and the emergence of leaves is important for the water balance of the basin since there are still no transpiration losses and the possibility of surface runoff is greater, which contributes to the reservoir supply. According to Pinheiro et al. (2016) the annual loss through evapotranspiration in the area is 70% of the precipitated water. On the other hand, at the beginning of the rainy season, part of the precipitated water is used to fill the soil macropores created by the roots during the dry season.

Leaf emergence begins with a stem moisture of 0.32 $m^3.m^{-3}$ (Figure 7), reaches its maximum level (around 1.0 $m^2.m^{-2}$) with a stem moisture of 0.34 $m^3.m^{-3}$ (Figure 6) and remains this way until the wet-dry transition occurs, when the leaves begin to senesce. Pinheiro et al. (2016), used remote sensing and field data, and gauged an average LAI of 0.97 $m^2.m^{-2}$ for the same area during the rainy seasons from 2004 to 2012. De Almeida et al. (2019), employed litter data and determined a maximum LAI of 3.47 $m^2.m^{-2}$ for the years 2014 to 2016 in the AEB.

Figure 7 – Correlations between stem moisture in catingueira, soil moisture and leaf area index (LAI)

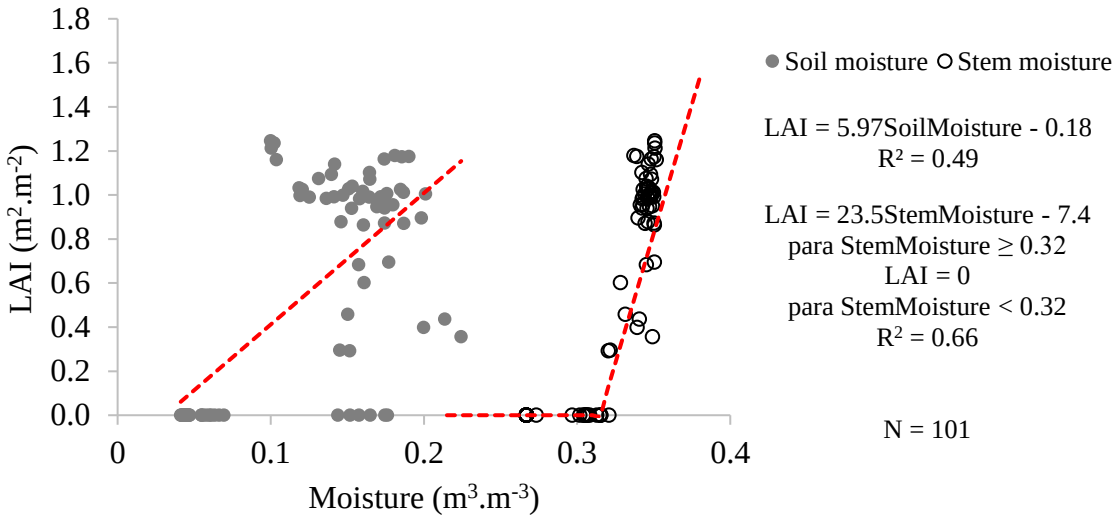

Soil and stem moisture also showed a good correlation between them (Figure 8) through a segmented fit equation that makes it possible to obtain stem moisture data in Caatinga areas where only soil moisture is available. Both in Figure 6 and in Figure 8 stem moisture reveals levels of constancy.

From a soil moisture of 0.08 $m^3.m^{-3}$ on, stem moisture becomes practically constant and shows no significant increase in plant moisture even with a soil moisture rise. This value is below the moisture level of the soil established as a permanent wilting point (PWP) of 0.11 $m^3.m^{-3}$ (COSTA et al., 2016). Here it can be seen that catingueira plants are able to maintain themselves at a potential stem moisture level even in a soil moisture defined by literature as one in which cultivated plants are no longer able to absorb water. It is important to highlight in this context that soil water content in the PWP is determined at a pressure of -1.5 MPa, because from this value on (lower matrix potentials) the water content in the soil varies very little. This means that the available water hardly changes below this point. The tree species clearly demonstrates its considerable adaptive capacity for water absorption; its PWP would possibly occur at potentials close to -4.0 Mpa. Figure 8 also shows the points of residual moisture (RM) (minimum moisture maintained by the soil) and field capacity (FC) (maximum capacity of water retained by the soil). It can be seen that the soil did not reach either of these two extremes during the study period.

Figure 8 – Correlation analysis between stem moisture in catingueira and soil moisture in the root zone

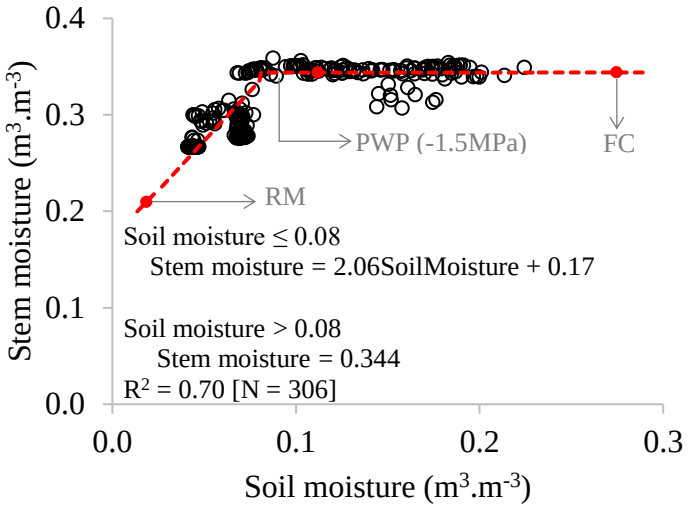

RM – residual moisture, PWP - permanent wilting point and FC – field capacity.

The historical average of precipitation in the EBA amounts to 583 mm (COSTA et al., 2021).). During the evaluated period, the rainfall measured in the rainy season was lower than the climatological normal and totaled 440 mm. It could still be observed that within the rainy season the plants were able to reach their potential humidity of approximately 0.36 $m^3.m^{-3}$, the level of humidity obtained during the saturation process of the samples for the sensor calibration (Figure 3b). This way it may be inferred that a reduction in precipitation does not influence the water storage capacity of the plants, but the persistence of this capacity for a longer period of time during the year, since in rainier years the tendency is for the soil to remain moist for a longer period of time.

The plant moisture data associated with sap flow velocity are presented in Figure 9 for the rainy and the dry season. Catingueira has low stem moisture at dawn (Figure 9a) and, according to Dombroski et al. (2011), also has low leaf water potential in this period. It may be observed that there is a positive variation in stem moisture from 9:00 am on in the rainy season, possibly due to a greater extraction of water from the soil to supply the later transpiration needs of the plant.

Water supply in the stem starts with a downward sap flow. This means that water is translocated from higher plant structures to the stem. On some days the sap flow only becomes positive at the beginning of the night, e.g. on 04/19/2021 (rainy day: 24 mm) and 04/20/2021, while on 04/21/2021 it already starts to be positive between 9 am and 10 am. It is

interesting to observe that sap flow velocity presents peaks with a frequency of 19h between them. This frequency is also observed for valleys (minimum points) and some specific levels.

Figure 9 – Hourly data of stem moisture (gray) and sap flow velocity (black) in the rainy (a) and the dry (b) period on three consecutive days, as well as the hourly average for the referred periods.

Figure 9 – Hourly data of stem moisture (gray) and sap flow velocity (black) in the rainy (a) and the dry (b) period on three consecutive days, as well as the hourly average for the referred periods

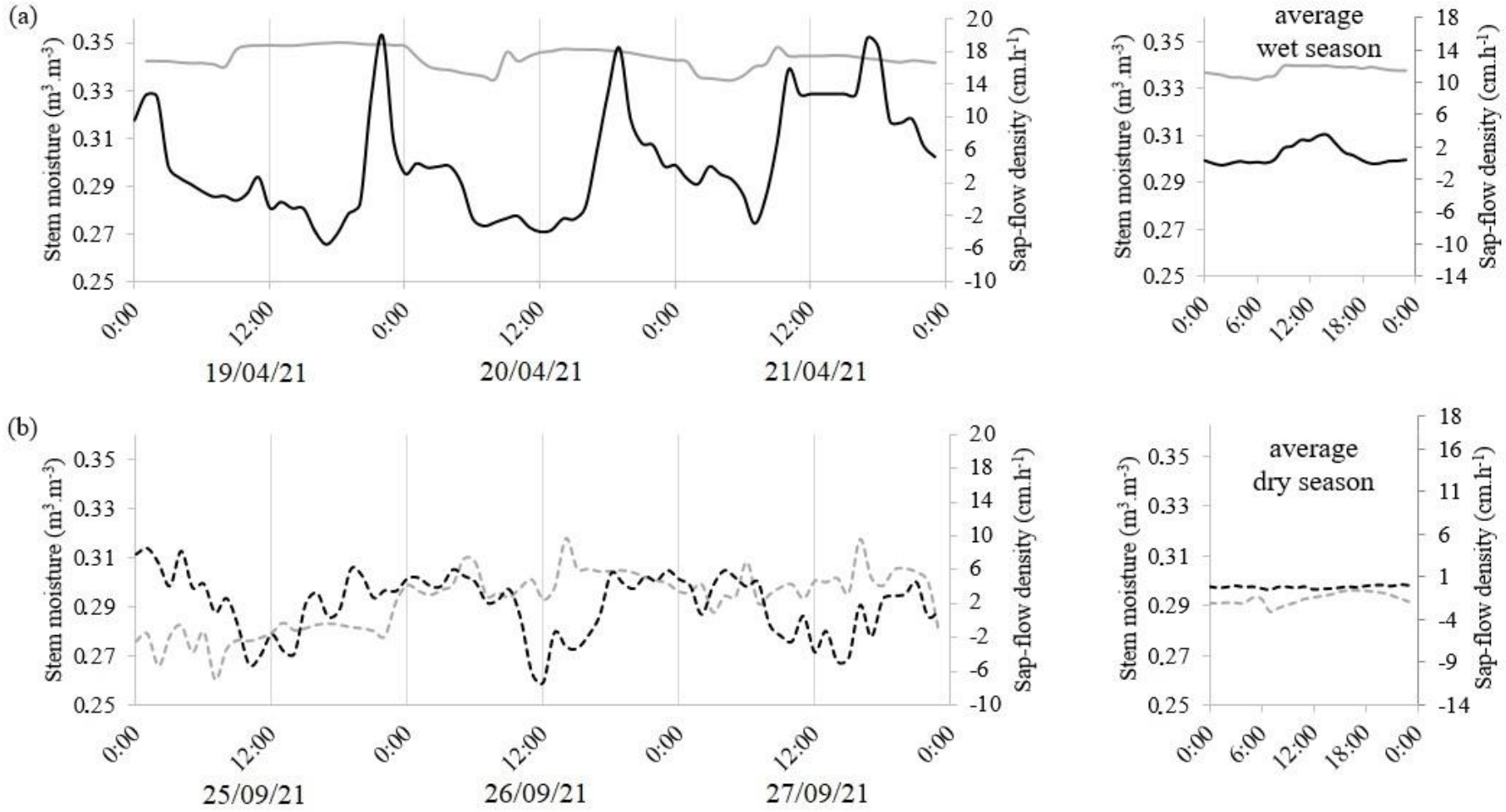

According to average values, there is less sap flow at night and even some negative (descending) flow, which corresponds to the hours of lower stem moisture and higher soil moisture. This fact, combined with the observation of daily variation in soil moisture even in the dry stage when there is no water input from rain, leads to the belief that there may be a release of water from the roots to the soil during these times. The values of stem moisture and sap flow are lower during the dry period (Figure 9b), especially during intervals of greater atmospheric water demand close to 12:00. Although plants are without leaves in most of the dry season and, therefore, the absorption of water by the plant in this period reflects more its need for survival, than its development and transpiration processes, the catingueira still has leaves in the beginning of the dry period. Stem moisture does not show a well-defined daily behavior pattern in this period.

2.4 Conclusions

This work made it possible to identify soil and stem moisture levels that allow leaf increment at the beginning of the rainy season. There is a delay of approximately 10 days until the beginning of leaf production in the rainy season; in relation to the increase in soil and stem moisture, the emergence of leaves starts with stem moisture only 3% above annual average. The leaf area index reaches its maximum level when stem moisture is 10% higher than the annual average.

Catingueira trees (*Caesalpinia pyramidalis* Tul.) are able to absorb water from the soil, even though the soil has a water potential below that commonly identified as permanent wilting point (-1.5 Mpa). The stored volume of water in plants represents an important part of the water storage in a watershed: Only in the catingueira plant, the volume of stored water represents 108% of the average volume observed in the Boqueirão reservoir during the study period.

3 SAP FLOW IN SEASONALLY DRY TROPICAL FOREST

Abstract: The assumption of the soil-plant-atmosphere continuum is that the movement of water occurs through the plant from areas of high to areas of low water potential, and in some cases, there may be an inverse flow of sap. Thus, the objective was to analyze the dynamics of sap flow in typical plants of the Caatinga biome (*Caesalpinia pyramidalis* Tul.), with in situ measurements, in two water regimes, rainy and dry, in order to verify the existence or not of inverse flow. The experiment was carried out on plants of *Caesalpinia pyramidalis* Tul., in a seasonally dry tropical forest area. The sap flow method used was the heat ratio (HRM) using thermocouple sensors and a heating probe. It was identified that catingueira plants have the ability to perform inverse sap flow at night and predawn basically throughout the year. Higher sap flow was observed in the transition seasons due to atmospheric conditions and soil moisture. There was a superiority of 46% of the catingueira sap flow in the rainy season compared to the dry season. It was noticed that the nocturnal sap flow is more significant in the driest months, demonstrating another adaptive strategy of the species.

Keywords: Heat ratio method, Caatinga, vapor pressure deficit

3.1 Introduction

Evapotranspiration (ET) is a hydrological process that still needs further understanding, especially in semi-arid regions. The magnitude of this process can represent 95% of the water balance in dry areas (WILCOX; BRESHEARS; SEYFRIED, 2003) and, in general, governs the availability of water resources, agricultural productivity and irrigation efficiency, in addition to impacting the severity of droughts, floods and forest fires (LITTELL et al., 2016; MOLDEN et al., 2010). The individual components of ET include plant transpiration (T) and soil evaporation (E), and in some cases it is also considered the evaporation of water intercepted by the vegetative canopy and the litter layer under the soil (KOOL et al., 2014).

The partitioned analysis of water flows in vegetative systems is able to provide valuable information about the individual magnitude of the processes, since the evaporation and transpiration factors differ in their responses to environmental conditions. In arid regions, the evaporation factor is potentially substantial due to the high atmospheric demand represented by potential evapotranspiration (ET_o) (KOOL et al., 2016), while transpiration can be reduced through plant adaptation mechanisms (DOMBROSKI et al., 2011). Transpiration is governed by the flow of sap in the plant and in relation to this factor, until the present moment, the studies conducted to quantify it in preserved Caatinga vegetation are incipient, especially considering the unique hydrological processes that occur in this region, given the deciduous and physiological adaptations of Caatinga plants.

The assumption of the soil-plant-atmosphere continuum (SPAC) is that water movement occurs through the plant from areas of high to areas of low water potential (Ψ). Soil water uptake by plants occurs when there is a conduction gradient for water loss through transpiration due to a large difference between the low water potential of the dry atmosphere and the relatively high water potential of the leaves(GOLDSMITH, 2013). This gradient is propagated through the plant along a continuous water column that is under tension, resulting in water uptake that occurs at high soil water potentials (NOBEL, 2009).

Furthermore, as soil water is generally considered to be the only readily available source of water for plants, transport of water through the soil-plant-atmosphere continuum (SPAC) is considered unidirectional from soil to atmosphere via roots, stems, and leaves (TYREE; ZIMMERMANN, 2002). However, studies (CASSANA et al., 2016; ELLER; LIMA; OLIVEIRA, 2013; GOLDSMITH; MATZKE; DAWSON, 2013) demonstrate that water can move from the humid atmosphere during leaf wetness events to the dry plant by foliar absorption of water, while also moving from the wet soil to the dry plant, supplying the plant,

then, in two ways (GOLDSMITH, 2013). In addition, it is possible that on certain occasions water may also move from the humid atmosphere, during foliar wetness events, to dry soil by foliar water absorption (ELLER; LIMA; OLIVEIRA, 2013; GOLDSMITH, 2013; HAO et al., 2010). Another possibility is that the plant is supplied with water, but that this is not lost to the atmosphere, due to stomatal closure, in this way the water potential gradient in the soil will drive water through the root system from wetter layers to drier layers (FERREIRA et al., 2018; YU et al., 2013).

Despite the considerable advances made on the subject, it is still unclear how certain physiological characteristics influence plant survival during drought, especially in tropical and semiarid ecosystems. The results obtained through the reviewed works on the subject provide the impetus to investigate whether these processes occur in the Caatinga biome, which would justify the survival of plants under conditions of long periods of water scarcity.

In this context, the objective is to analyze the dynamics of the sap flow in typical plants of the Caatinga biome (*Caesalpinia pyramidalis* Tul.), with in situ measurements, in two water regimes, rainy and dry, in order to verify the existence or not of inverse flow.

3.2 Materials and Methods

3.2.1 Study area

The study area is the Aiuaba Experimental Basin (AEB, 12 Km²), entirely composed of preserved Caatinga and located in the municipality of Aiuaba (DE ARAÚJO; PIEDRA, 2009). AEB has its drainage network composed of two main intermittent streams controlled by the Boqueirão reservoir (60 thousand m³) (Figure 1). It is part of the Alto Jaguaribe River Basin, in the region of the State of Ceará called Inhamuns.

Figure 1 - Location map of the study region and instrumentation of the Aiuaba Experimental Basin (AEB)

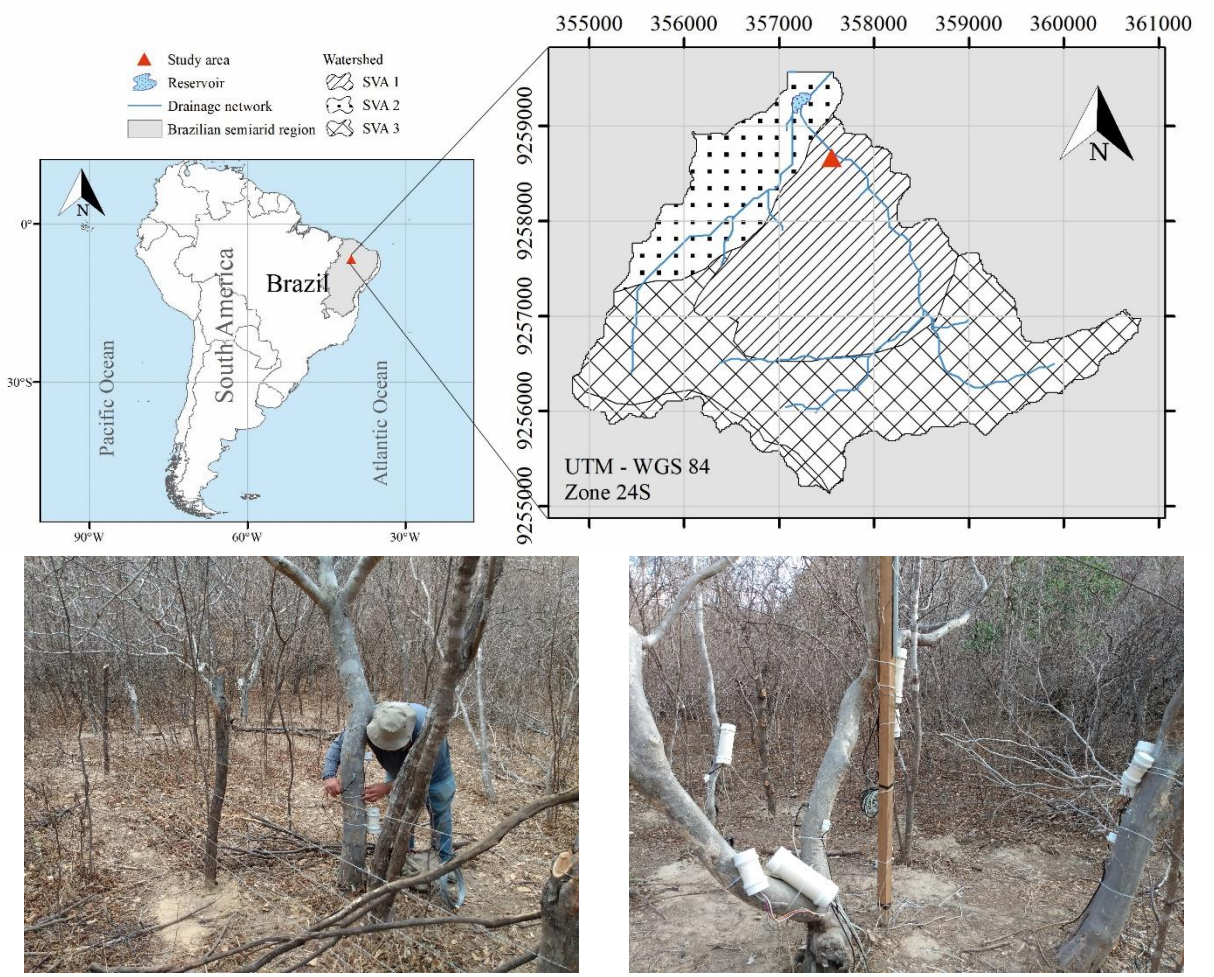

The basin is located in the southwest sector of the Aiuaba Ecological Station (ESEC). Established in 1978, the Aiuaba ESEC is associated with the maintenance of the flora and fauna biodiversity of the caatinga biome and plays an important role in the region's hydrological cycle, mainly due to its dense forest cover (DE ARAÚJO; PIEDRA, 2009). AEB is divided into three soil-vegetation associations (SVA). The first association (SVA1) occupies

20% of the area with Chromic Luvissol type soil and the depth of the root zone of the plants is 80 cm. The Second System (SVA2) occupies 34% of the area, presents soils classified as Red-Yellow Argisol and the average depth of the root zone is 60 cm. SVA3, which has 46% of the basin area, has Litholic Neosol soil, and a rooting depth of 40 cm (COSTA et al., 2016; PINHEIRO et al., 2016).

AEB has been monitored since January 2003 by HIDROSED - Grupo de Pesquisa Hidrosedimentológicas do Semiárido <www.hidrosed.ufc.br>. The studies carried out in the basin during this period include measurements and analyzes of hydrological variables, such as precipitation, evaporation, surface runoff and losses from plant interception (DE ARAÚJO; PIEDRA, 2009; DE FIGUEIREDO et al., 2016; MEDEIROS; DE ARAÚJO; BRONSTERT, 2009) and hydrogeological and sedimentological studies (ARAÚJO, 2012; COSTA et al., 2013, 2016; PINHEIRO et al., 2016; PINHEIRO; VAN LIER; METSELAAR, 2018), among others.

The climate of the region according to the Koppen classification is BSh (tropical semi-arid), with annual potential evaporation of 2500 mm, average annual precipitation of 549 mm and average annual temperature of 26 ºC (PINHEIRO et al., 2016).

3.2.2 Study installation

The field experiment was installed at SVA1 during the period from 11/03/2018 to 11/03/2021. The study began with a monitored plant and was expanded over the years (Table 1) ending with two monitoring sectors, containing two to four plants in each. The division optimized the supply of energy, through solar panels, to the systems. The data collection and storage system were carried out through dataloggers developed using Arduino, an open source electronic platform based on hardware and software.

Table 1 – Catingueira trees monitored over the years and hydroactive xylem area data

Start of monitoring		Plant	DSH*	Stem area	Xylem area
Month	Year		(cm)	(cm^2)	(cm^2)
11	2018	Tree 1	15.29	183.61	70.33
8	2019	Tree 1	15.31	184.11	91.54
		Tree 2	13.75	148.51	77.13
		Tree 3	16.01	201.34	98.31
11	2020	Tree 1	15.34	184.88	91.85
		Tree 2	14.29	160.43	82.02
		Tree 3	16.33	209.42	101.44
		Tree 4	11.01	95.47	54.19
		Tree 5	16.23	206.98	100.50
		Tree 6	5.41	23.00	17.43

*DSH – Tree diameter at sensor installation height (~1,20 m).

3.2.3 Heat Ratio Method (HRM) for estimating sap flow

Six catingueira plants (*Caesalpinia pyramidalis* Tul.) were chosen as representative species of the study area to be monitored for sap flow. These species were chosen according to the phytosociological survey carried out in the study area (Table 2). A variety of species is observed in the study site, however, the Marmeleiro and Catingueira are the two most representative species. Both are deciduous. However, the quince tree is a small shrub species, with a small stem diameter, while the catingueira is the tree species with the highest absolute density in the area. Therefore, it was the species chosen for monitoring the SPAC.

Table 2 - Phytosociological parameters of the species sampled in the SVA1 of the Aiuaba Experimental Basin

	Common name (scientific name)	AD	RD (%)
1	Marmeleiro (*Croton sonderianus* Muell. Arg.)	2680	77,3
2	Catingueira (*Caesalpinia pyramidalis* Tul.)	256	7,4
3	Planta Morta	179	5,2
4	Cipó (*Combretum laxum*)	107	3,1
5	Frei Jorge (*Cordia trichotoma* (Vell.) Arrab.ExSteud)	99	2,9
6	Rompe Gibão (*Bumeliaobtusifolia Humb.* Ex Roem. &Shult.)	56	1,6
7	Pau Mocó (*Luetzelburgia auriculata* (Allemão) Ducke)	21	0,6
8	Feijão Bravo (*Cynophalla flexuosa* (L.) J.Presl)	14	0,4
9	Jurema Branca (*Mimosa ophthalmocentra* Mart. exBenth)	14	0,4
10	Violeta (*Dalbergia Cearensis* Ducke)	14	0,4
11	Guaxuma (*Helicteres guazumifolia* Kunth)	7	0,2
12	Juazeiro (*Zizyphus joazeiro* Mart.)	7	0,2
13	Jurema Preta (*Mimosa tenuiflora* (Willd.) Poir.)	7	0,2
14	Maniçoba (*Manihot glaziovii* Müll. Arg.)	7	0,2

AD - Absolute density (ind.ha^{-1}), RD - Relative density (%).
Source: (TILESSE et al., 2021).

The sap flow method used was the heat ratio (HRM) method developed by Burgess et al. (2001). This method measures the rate of increase in temperature, following the release of a heat pulse, at equidistant points downstream and upstream of a heating probe. The heat pulse velocity (Vc, cm h^{-1}) is calculated as (Equation 1):

$$Vc = \frac{4kt \ln\left(\frac{v_1}{v_2}\right) - x_2^2 + x_1^2}{2t(x_1 + x_2)} \beta 3600 \quad (1)$$

Where: k is the thermal diffusivity of fresh wood (cm.h^{-1}), x_1 and x_2 are the corrected distances (cm) between the heater and the temperature probe, and v_1 and v_2 are temperature increases

(relative to the initial temperatures) at equidistant points downstream and upstream, respectively, and t is the measurement time (s).

The system, composed of three probes, two of them positioned upstream and downstream of the heating probe at a distance of x = 0.6 cm (Figure 2), contains a copper-constantan thermocouple positioned in the centre of a 1.5 cm long hypodermic needle. The heating probe, also composed of a hypodermic needle of the same size, was surrounded by an electrical resistance (constantan wire). The heat pulse is 10 s, released every 10 min, at a voltage of 12V.

Figure 2 – Scheme showing details of the probes (A) and installation on the catingueira stem (B)

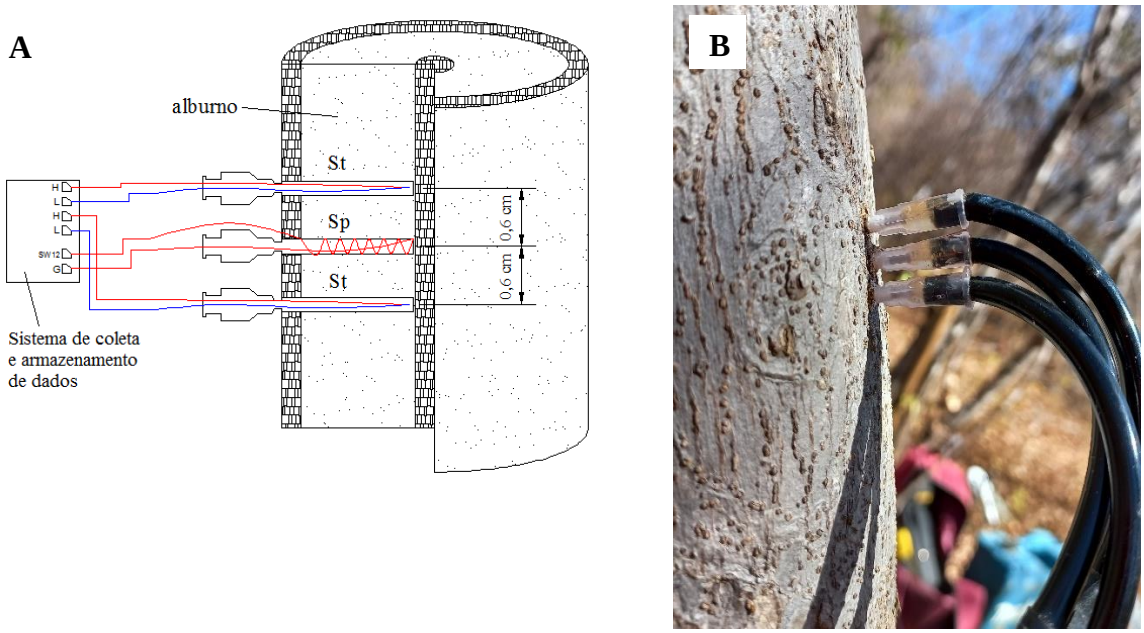

St – thermocouple probe; Sp – Heat pulse probe; red wires are constantan and blue wires are copper.

Thermal diffusivity (k) is given a nominal value of 2.5×10^{-3} cm^2 s^{-1} (MARSHALL, 1958). Installing sensors in xylem tissue causes substantial mechanical damage. In addition to the interruption of flow paths by the insertion of probes, intact vessels can become occluded, as the plant responds to injury by forming tyloses. The resulting region of non-conductive wood around the probe insertion site affects the Vh measurement by decreasing the v1/v2 ratio. To correct this error, we use the coefficient β admitted as 1.7023 by Burgess et al. (2001) for a probe insertion diameter of 0.17 cm.

Even with careful placement of the probes, the spacing between them is likely to be at least a little asymmetrical. In this way, the positioning of the probe must be corrected according to Equation 2 (BURGESS et al., 2001).

$$x_2 = \sqrt{\left(4kt \ln\left(\frac{v_1}{v_2}\right) + x_1^2\right)} \quad (2)$$

Where: x2 denotes the incorrectly spaced probe, x1 is assumed to be correctly spaced at 0.6 cm and t is the measurement time.

Since it is not known which probe is positioned incorrectly, one can solve Equation 2 by assuming that x1 is positioned correctly. The ratios between v1 and v2 (v1/v2) will approach an ideal value asymptotically, with the rate of change decaying exponentially with time after the heat pulse. Thus, Burgess et al. (2001) suggests that measurements should be taken at least 60 s after the heat pulse has been released. As v1/v2 is effectively linear between 60 and 100 s, the value of these average proportions was different from a representative value measured at the median time of 80 s by <0.4% for extreme cases, although generally the difference was negligible.

Only a portion of the xylem tissue (the sapwood, hydroactive xylem) contains moving sap. Heat pulse probes effectively measure a weighted average of the velocities of moving sap and "stationary" wood. The sap velocity (Vs) can be determined by measuring the fractions of sap and wood in the xylem and considering their different densities and specific heat capacities (Equation 3).

$$V_s = \frac{Vc\rho_b(C_w + m_c C_s)}{\rho_s C_s} \quad (3)$$

Where: Vc is the corrected heat pulse velocity ($cm.h^{-1}$), ρb is the basic density of the wood (dry weight/green volume, in $kg.cm^{-3}$), cw and cs are the specific heat capacity of the wood. wood matrix (1200 $J.kg^{-1}.°C^{-1}$) and sap (4182 $J.kg^{-1}.°C^{-1}$), respectively, mc is the water content of sapwood and ρs is the water density ($kg.cm^{-3}$).

The volumetric flow of the sap can be obtained as the product of the sap velocity (Vs) and the cross-sectional area of the hydroactive xylem. For the calculation of the hydroactive xylem area (sapwood) we used the allometric equations, specific for the species, developed by Tilesse et al. (2021).

3.2.4 Monitoring soil and stem moisture

Both soil and stem moisture were monitored using low-cost capacitive sensors (ARAÚJO et al., 2021). These have metal rods as electrodes, so variations in the dielectric constant and electrical resistance of the rod also change the frequency of an oscillator (integrated circuit 555) that is read by an Arduino Pro-Mini board and transmitted via serial communication. Two sensors were installed, at 20 and 40 cm depth, in the root zone of the catingueira plants and another one in the stem of the same tree.

3.2.5 Obtaining the vapor pressure deficit (VPD)

The vapor pressure deficit (VPD) is the difference between the maximum pressure that can be exerted by the water vapor (saturation pressure) and the pressure being exerted by the amount of water vapor in the air at a given instant (current pressure) (AMARAL et al., 2020). This difference is a measure of the evaporating power of the air, having a direct relationship with the processes of evaporation and transpiration, since these depend on the vapor pressure gradient between the evaporating surface and the air, among other factors. The vapor pressure deficit (VPD) can be calculated by the following equation (Equation 7):

$$\text{VPD} = e_S - e_a \tag{7}$$

Where: VPD is the vapor pressure deficit (kPa), es is the saturation vapor pressure (kPa), and ea is the actual vapor pressure (kPa).

Vapor saturation pressure (eS) represents the amount of vapor that can exist in a given atmosphere as a function of temperature, the vapor saturation pressure can be calculated (in kPa), knowing the air temperature (Ta in ºC), through the Tetens Equation 8:

$$e_S = 0{,}6108 \times 10^{\frac{7{,}5 \times T_a}{237{,}3+T_a}} \text{ para Ta} \geq 0\ ℃ \tag{8}$$

Where: es is the saturation pressure (kPa), Ta is the air temperature (ºC).

The actual vapor pressure (ea) is obtained as a function of the average relative humidity (RHavg) and the vapor saturation pressure (s), through Equation 9.

$$e_a = e_S \times \text{UR}/100 \tag{9}$$

Where: ea is the actual vapor pressure (kPa), es is the saturation pressure (kPa) and RH is the relative humidity (%).

3.3 Results and Discussion

Figure 3 illustrates the proper functioning of the sensors located upstream (Vu) and downstream (Vd) of the heating probe right after the emission of a heat pulse. The sensors installed in plant 4 showed abnormal functioning, therefore, this replication was discarded from the sap flow calculations. It is noticed that the values of Vu and Vd increased in different proportions after the pulse, indicating the direction of the flow. At the time the test was performed, plant 5 had an inverse sap flow since Vd received more heat than Vu. The heat peaks are generally seen around 40 seconds after the pulse, except for plant 6, which has the smallest stem diameter of all (Table 1), producing faster heat conduction.

Figure 3 – Temperature increase verified by thermocouples positioned above (Vu) and below (Vd) the pulse probe seconds after the emission of a heat pulse

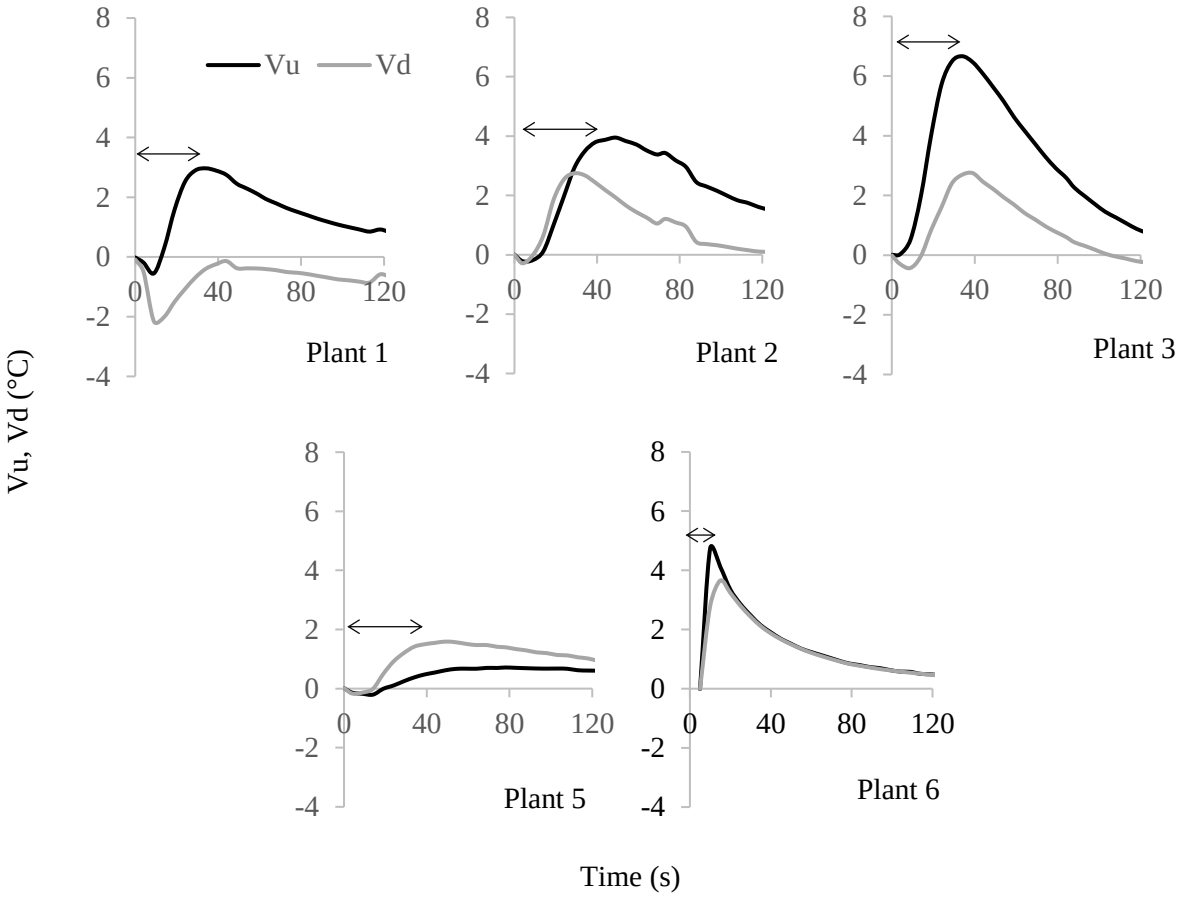

Through the daily behavior of the sap flow (Figure 4) it is noted that the catingueira plants are able to perform inverse flow as reported by Burgess and Dawson (2004), Cassana et al. (2016), Eller et al. (2013), Ferreira et al. (2018), Goldsmith et al. (2013) e Nadezhdina et al. (2010) in other species and biomes. In catingueira, this phenomenon occurs at times between 6

pm and 6 am, mainly in transition periods. The reverse flow in plants can occur either by the movement of water absorbed by the leaves and transported towards the roots or by the hydraulic redistribution of water within the plants. Regarding the absorption of water by the leaves, this can be facilitated by specialized structures, such as trichomes (ELLER; LIMA; OLIVEIRA, 2016; FERNÁNDEZ et al., 2014; LIMM et al., 2009; PINA et al., 2016) and the hydathodes (MARTIN; VON WILLERT, 2000), but even leaves without these structures can be permeable to water directly through the cuticle (ELLER; LIMA; OLIVEIRA, 2013, 2016) or through the stomatal opening (BURKHARDT, 2010; BURKHARDT et al., 2012).

Figure 4 – Mean hourly sap flow in catingueira and vapor pressure deficit (VPD) in the dry, dry-rainy, rainy and rainy-dry transition seasons

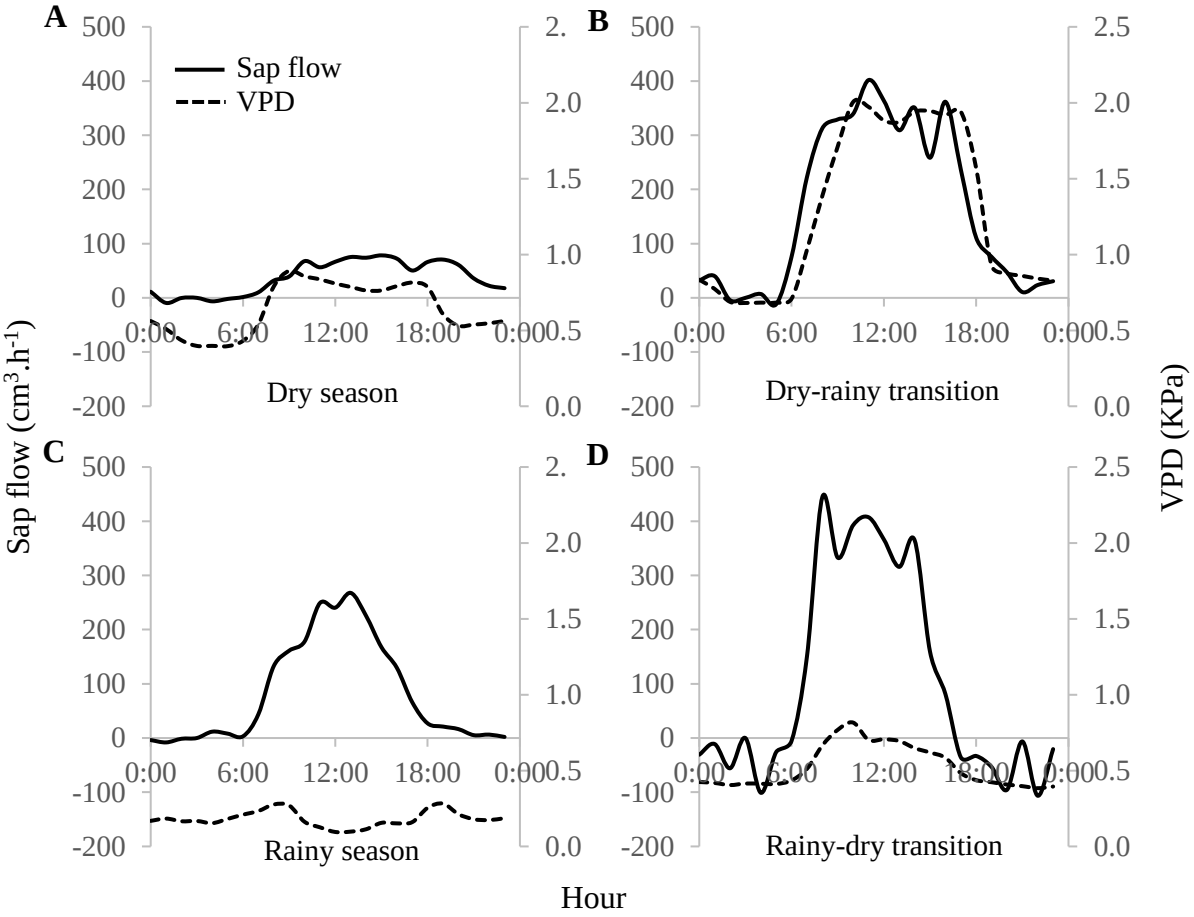

Whatever the means of entry, foliar water uptake is likely to be restricted to leaf wetness events, when atmospheric water potentials are normally very low (NOBEL, 2009), that is, the DPV is low, as observed in the present study. Only when water has agglomerated on the leaf surface and the leaf is experiencing a water deficit is it likely that the inner tissue of the leaf has less water potential than the boundary layer. The strongest evidence for foliar water

uptake comes from ecosystems affected by fog and dew, where wetting events occur when soil water availability is limited (ELLER; LIMA; OLIVEIRA, 2013; GOLDSMITH; MATZKE; DAWSON, 2013; LIMM et al., 2009). The average soil moisture in the study area is 0.06 $m^3.m^{-3}$ in the dry season and 0.14 $m^3.m^{-3}$ in the rainy season.

As there are several possible pathways for water entry into leaves, this water acquisition strategy has been observed in plants from various ecosystems (BERRY; WHITE; SMITH, 2014; CASSANA et al., 2016; ELLER; LIMA; OLIVEIRA, 2013, 2016; GOTSCH et al., 2014; MARTIN; VON WILLERT, 2000; PINA et al., 2016; SIMONIN; SANTIAGO; DAWSON, 2009). The water acquired by foliar absorption is considered of special ecological relevance in dry or seasonally dry environments, in which frequent leaf wetting events occur (OLIVEIRA et al., 2014).

Conditions in the plant that result in water movement from leaves to stem similarly require the presence of a conduction gradient, where foliar uptake of water results in a greater leaf water potential than that of the stem (GOLDSMITH, 2013a). Eller et al. (2013) demonstrated an increase in leaf water potential resulting from foliar water uptake, as well as an inverse stem water flow.

Although the catingueira is a deciduous species, which loses its leaves in the long dry period, remaining like this for an average of 5 months a year, there is another plant structure capable of absorbing water that is present in this species, the lenticels. Lenticels are in the epidermis of different plant organs, such as the stem, and are pores that always remain open, unlike stomata, which regulate their opening extent. Lenticels allow the exchange of gases between the environment and the internal tissue spaces of the organs (CARRILLO-LÓPEZ; YAHIA, 2019).

It is also noticed that in the transition seasons (Figures 4B and 4D) the sap flow has a greater amplitude, this fact can be explained because in these periods of the year the vapor pressure deficit is greater than in the rainy season and there is more moisture in the soil than in the dry season.

Figure 5 shows a better configuration to elucidate the relationship between catingueira sap flow and vapor pressure deficit. There is a correlation between these two processes of 0.36 and 0.37 in the rainy and dry seasons, respectively. In addition, the daily peaks and valleys of sap flow and VPD correspond, evidencing the relationship between them. Studies like that of Amaral et al. (2020) demonstrate a high temporal correlation between sap velocity and VPD with fast responses. However, this experiment was carried out under controlled environmental conditions and without water deficit, different from the environmental

conditions of our study. Even so, it is observed that there were no delays in the responses of the sap flow to the VPD.

Once again, regardless of the period of the year, reverse flow events occur in catingueira. The average daily flow in the dry season in the catingueira is 890 $cm^3.h^{-1}$ while in the rainy season it is 1900 $cm^3.h^{-1}$, 46% higher. It is known that not all water that passes through the cross section of the stem where the sensor is located is transpired, but that there is a strong correlation between these two phenomena. However, it can be seen that even in the period when the plants do not have transpiring leaves, given their deciduous leaves in the dry period, there is still a large movement of water inside.

Figure 5 – Sap flow (continuous line) and vapor pressure deficit (VPD) (dotted line) on ten days of the 2019 rainy season (A) and ten days of the 2021 dry season (B)

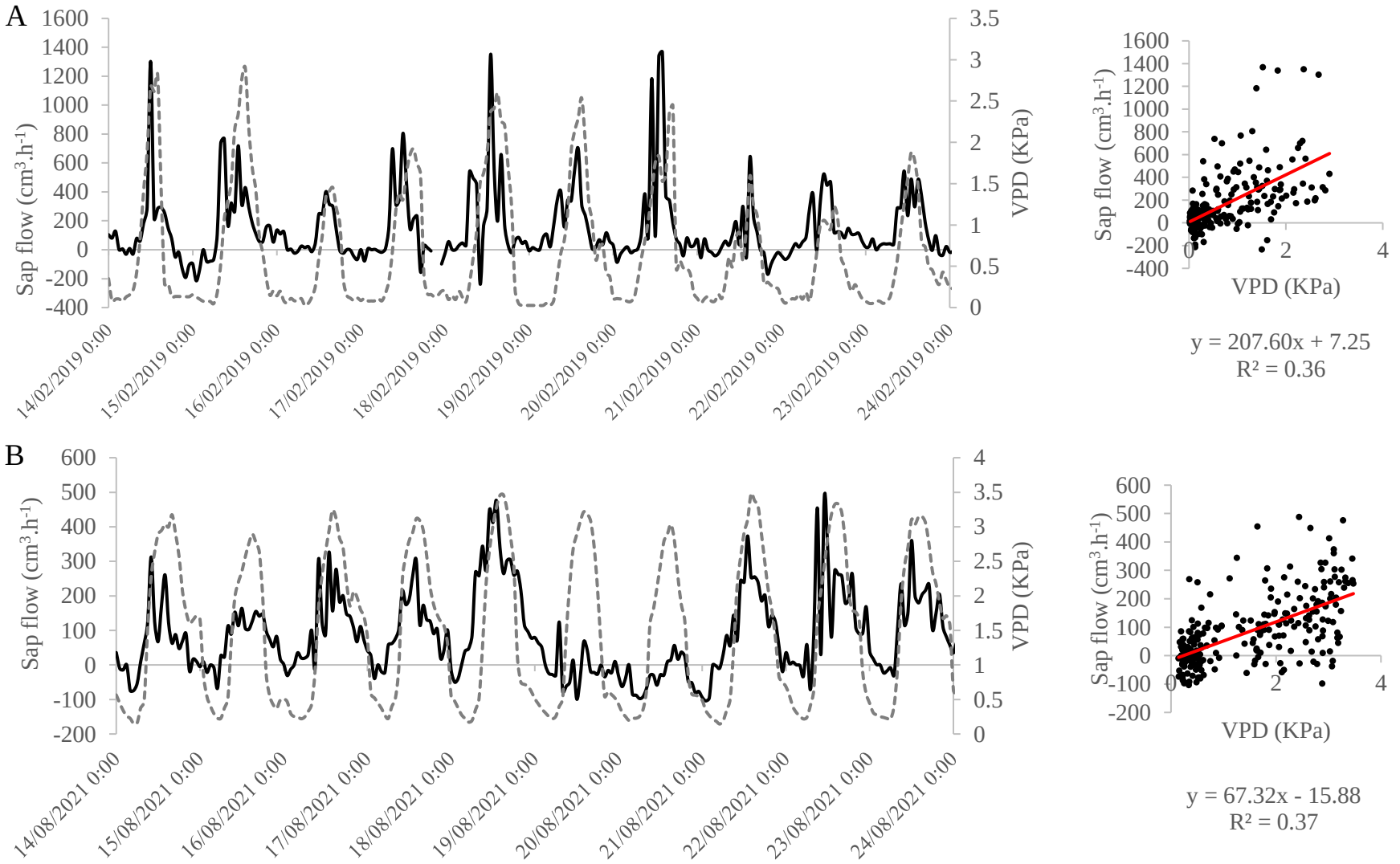

The annual rainfall of the years studied was 228.00 mm (2018), 391.41 mm (2019), 622.03 mm (2020) and 420.00 mm (2021). Thus, only the year 2020 was above the historical average of 549.00 mm (PINHEIRO et al., 2016). Figure 6 shows the relationship between the diurnal and nocturnal sap flow. It is observed that the months of greatest sap flow are the transition months (May and December). The highest percentages of night flow are among the driest months of the year. During this period, plants tend to avoid water loss as much as possible. Stomatal opening overnight would be a strategy. However, in this period the plants do not have leaves. Which raises the question about the use of water moved during the night.

Figure 6 – Daytime and night time sap flow and percentage of night time sap flow over the months of the year

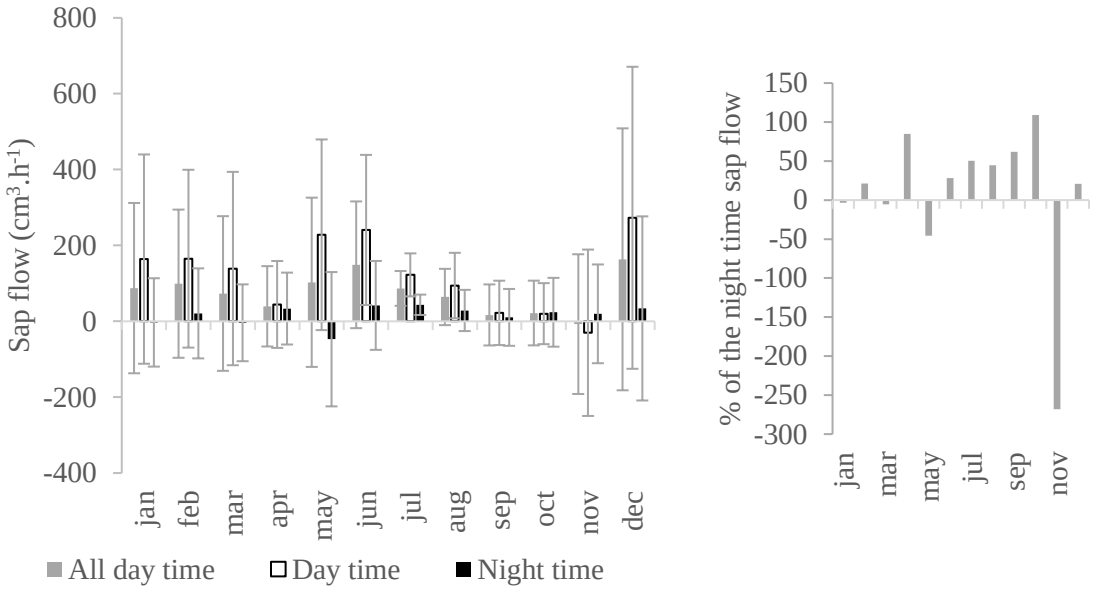

3.4 Conclusions

It was identified that catingueira plants (*Caesalpinia pyramidalis* Tul.) have the ability to perform inverse sap flow at night and predawn basically throughout the year. The highest sap flow occurs in transition seasons due to atmospheric conditions and soil moisture. There is a positive linear relationship between sap flow and vapor pressure deficit and the relationship between daytime and night time sap flow over the months of the year. It was noticed that the nocturnal sap flow is more significant in the driest months of the year due to the high daytime atmospheric demand in this period, which demonstrates another adaptive strategy of the species.

4 TEMPORAL DYNAMICS OF EVAPOTRANSPIRATION IN SEMIARID NATIVE FORESTS IN BRAZIL AND SPAIN USING REMOTE SENSING

Abstract: Evapotranspiration (ET) plays an important role in integrated water resource planning, development and management. This process is particularly relevant in semiarid regions. The aim of this study is, hence, to compare spatial and temporal patterns of actual evapotranspiration, as well as the temporal trends in two different semiarid forests, Caatinga (Brazil) and Tierra de Pinares (Spain). We used the Surface Energy Balance Algorithm for Land (SEBAL) to assess actual evapotranspiration (ETa) in both areas. In the Brazilian semiarid forest, Caatinga is the main vegetation, while it is Pinares in Spain. For this purpose, 69 Landsat-5 and 42 Landsat-8 images (1995 – 2019) were used. The Mann-Kendall test was applied to assess the occurrence of trends in precipitation, temperature and potential evapotranspiration data; and the Temporal Stability Index (TSI) to know which areas have greater seasonal ET_a. The annual amplitude of the potential evapotranspiration (ET_0) is the same in both areas, however, the Caatinga values are higher. In the Caatinga forest, when ET_0 presents its highest values throughout the year, ET_a presents the lowest, and vice versa. In the Pinares forest, ET_a follows the ET_0 dynamics during the year, and the difference between ET_0 and ET_a is maximum during the summer. The Caatinga forest showed a greater spatial variation of ET_a than the Pinares forest as well as a greater extension with lower temporal stability of ET_a than the Pinares forest. Both the Caatinga forest and the Pinares forest showed significant positive trends in annual ET_0 and ET_a. We estimate that the value of ET_a increases more rapidly in Pinares than in the Brazilian Caatinga. Taking Caatinga as a hydrological mirror, some consequences are expected to Pinares, such as significant changes in the water balance, increase of biodiversity vulnerability, and reduction of water availability in soil and reservoirs.

Keywords: SEBAL; Landsat; Caatinga; Tierra de Pinares; energy balance; drylands

4.1 Introduction

The continuous increase in water demand is a subject of concern (BORETTI; ROSA, 2019; COSGROVE; LOUCKS, 2015) and demands efficient management systems, particularly in semiarid regions (SUN et al., 2019). Those regions account for 15% of the global land area and feed 14% of the global population. Besides, semiarid ecosystems are very fragile and sensitive to climate change (SAFRIEL; ADEEL, 2005).

The Brazilian semiarid zone is characterized by an extremely negative atmospheric water balance - aridity index is below 0.50 (precipitation/potential evapotranspiration) (MARENGO et al., 2020) - and a considerable spatial and temporal variability in water supply. This area, near the Equator in the Southern Hemisphere, presents annual periods that are determined mainly by the precipitation rate: rainy and dry seasons (DE ARAÚJO; PIEDRA, 2009; DE FIGUEIREDO et al., 2016; PINHEIRO et al., 2016). These features contrast with other semiarid areas, such as the Spanish Northern Plateau, where precipitation distribution is relatively uniform throughout the year (CALAMA et al., 2019), and where the vegetation is mostly influenced by temperature. These marked seasonal differences may lead to a distinct spatial and temporal behaviour of the actual evapotranspiration (ET_a) in those semiarid areas.

Evapotranspiration (ET) is one of the most challenging components of the water balance equation to be measured (CASTELLI et al., 2018). It can be quantified using lysimeters or aerodynamic methods (e.g., Bowen ratio and Eddy Covariance), but such methods only represent the specific area around the experimental setup. The spatial variation of evapotranspiration on a large scale can be better captured by models based on remote sensing (JAAFAR; AHMAD, 2020). The high spatial resolution and long registration period of a USGS Landsat permits to assess a spatiotemporal ET series of vegetated and non-vegetated surfaces (CHEN; LIU, 2020; JAAFAR; AHMAD, 2020).

Thermal-energy balance models that use remote sensing, such as SEBAL (Surface Energy Balance Algorithm for Land), have been successfully applied to assess ET_a at field scale in many areas of the world. Teixeira, Bastiaanssen, Ahmad, and Bos (2009) applied SEBAL to estimate evapotranspiration in irrigated agriculture and Caatinga vegetation in the semiarid region of the São Francisco River basin, north-eastern Brazil; Losgedaragh and Rahimzadegan (2018) used it to compute evaporation from the freshwater bodies; the same authors (2018), as well as Rahimzadegan and Janani (2019), applied SEBAL to agricultural lands in a semiarid climate in Iran; Senkondo, Munishi, Tumbo, Nobert, and Lyon (2019) used it in a sub-tropical region in Tanzania's Kilombero Valley; whereas Gobbo et al. (2019) and Grosso et al. (2018) applied it to assess ET at irrigated and non-irrigated maize fields in Italy.

In the years to come, a significant reduction of precipitation and a temperature increase can be expected over global typical semiarid regions as a result of climate change (YANG et al., 2019). This trend may influence both the atmospheric and vegetation water demand, that is, the ET_a. Therefore, it is crucial and challenging to research for a better hydrological understanding of water-balance changes that may occur in semiarid ecosystems, such as Caatinga (Brazil) and Tierra de Pinares (Spain). The aim of this study is, hence, to compare spatial and temporal patterns of actual evapotranspiration, as well as to identify temporal evapotranspiration trends in both areas.

4.2 Materials and Methods

4.2.1 Study areas

The research took place in two forested semiarid areas (Figure 1). The Caatinga experimental area is located inside the Aiuaba Ecological Station (ESEC, 117 km²), a Federal preservation area located in the Brazilian Northeast. This space has been fully preserved since 1978 and monitored since 2003 by the Semiarid Hydro-Sedimentological Research Group (http://www.hidrosed.ufc.br/index.php).

Figure 1 - Geographical location of the study areas and meteorological stations: Caatinga forest in north-eastern of Brazil and Tierra de Pinares forest in Valladolid (Castile and Leon), Spain

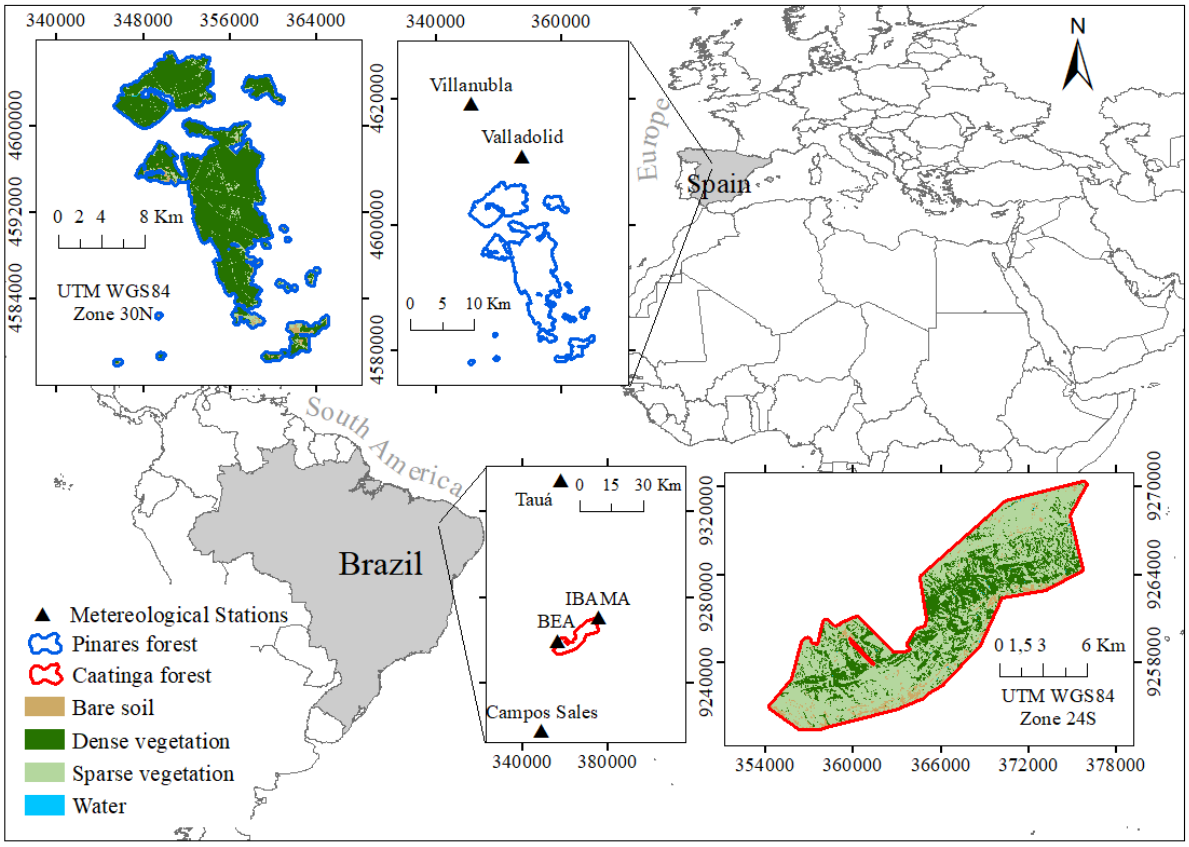

The Caatinga experimental area is part of the Jaguaribe River basin. According to the Köppen classification, the local climate is Bsh (hot semiarid) with potential annual evaporation of 2,500 mm, average annual precipitation of 549 mm, and average annual temperature of 26 ºC (PINHEIRO et al., 2016). The rainy season is concentrated from January to April (Figure 2a). The predominant lithology is the crystalline complex of metasedimentary formation. Soils in the region are generally shallow and originated from a crystalline substrate.

The predominant soil types are Luvisols, Latosols, and Argisols (DE ARAÚJO; PIEDRA, 2009; FARIAS et al., 2019).

Figure 2 - Climatic chart of the study areas: (a) Caatinga forest in Brazil and (b) Pinares forest in Spain

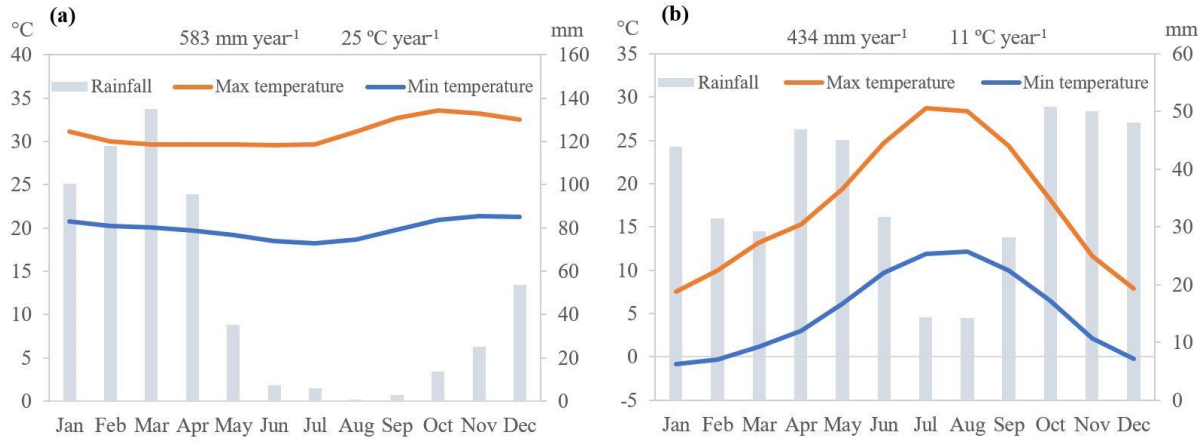

The Pinares forest (106 km^2) is located in Tierra de Pinares, in the province of Valladolid, Spanish Northern Plateau. Local vegetation there is formed mainly by stone pine (*Pinus pinea* L), but the maritime pine (*Pinus pinaster*) and holm oak (*Quercus ilex*) can also be found (BELLO, 2004). The soil is deep and sedimentary, with a sandy texture (more than 90% sand) and low water-holding capacity (CALAMA et al., 2019). Pinares forest has a continental Mediterranean climate which, according to the Köppen classification, is Bsk (cold semiarid). The annual rainfall is 434 mm and it is more regular throughout the year than in the Caatinga forest (Figure 2b). The annual mean temperature 11 °C (MORENO-FERNÁNDEZ et al., 2018), with a minimum mean temperature in winter close to 4 °C and a maximum mean temperature higher than 21 °C, and the potential annual evapotranspiration 1,100 mm (VICENTE-SERRANO et al., 2014). In the area, the confluence of the rivers Pisuerga and Duero takes place.

4.2.2 Satellite Imagery and Meteorological data

Actual evapotranspiration (ET_a) was estimated for the two experimental areas by using the imagery of Landsat 5 and Landsat 8. Landsat 5 captured images from March 1984 to January 2012 on six 30-m visible bands and a 120-m thermal band. Landsat 8 was launched in February 2013 and is still operating. Landsat 8 OLI images have eight 30-m bands, two 100-m thermal bands and a 15-m panchromatic band. In this study, all the available cloudless images

between 1995 and 2019 were used (Figure 3): 37 images of the Caatinga forest and 74 of the Pinares forest, totalling 111 images. The imaging time was 12:00 UTC (path 217 and row 65) for Caatinga, and 11:00 UTC (path 202 and row 31) for Pinares.

Figure 3 - Satellite data of the period from 1995 to 2019, used for the assessment of actual evapotranspiration in the Caatinga forest and the Pinares forest

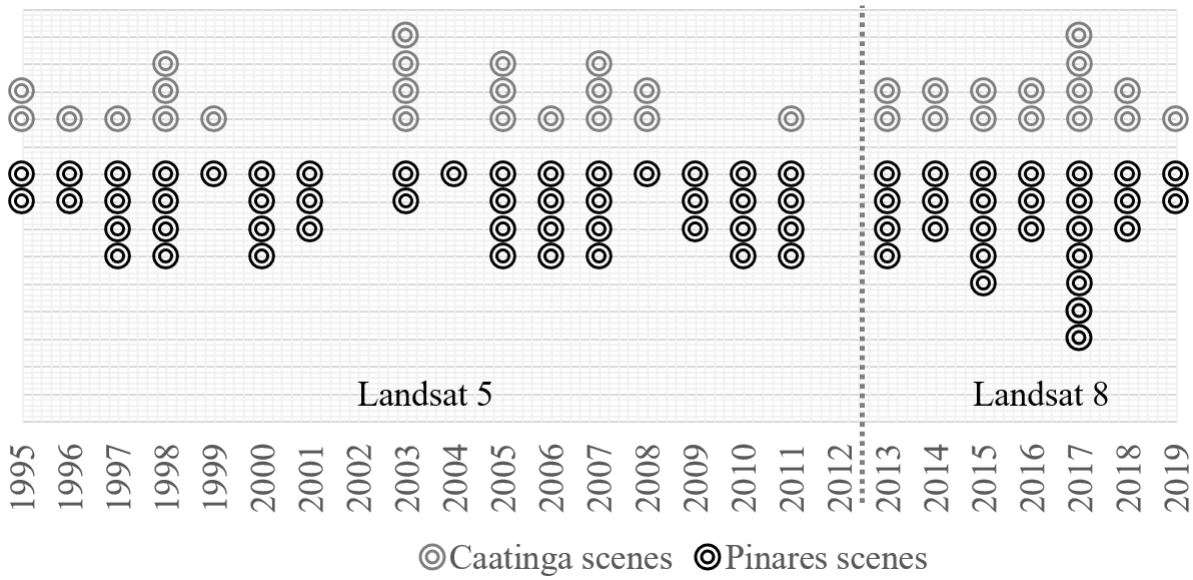

The Caatinga forest usually is excessively cloudy during the rainy season, so that practically no image was sufficiently clear (i.e., cloudless). During the rainy months, maximum cloud coverage was set to 10%, and the specific areas covered by clouds were disregarded.

Shuttle Radar Topography Mission (SRTM) images were employed to generate the Digital Elevation Model (DEM). Both Landsat and SRTM data were provided by the United States Geological Survey (USGS) (https://earthexplorer.usgs.gov/).

Daily and hourly field data of wind speed, temperature, relative humidity, solar radiation, air pressure and precipitation were obtained from the National Institute of Meteorology (INMET) and the Ceará Foundation of Meteorology and Water Resources (FUNCEME) for the Brazilian forest, and from the State Meteorological Agency (AEMET) for the Spanish forest. Table 1 shows the stations and periods of available data.

Table 1 - Synthesis of meteorological data obtained for the Caatinga forest and the Pinares forest

Area	Station	Agency	Latitude	Longitude	Data	Period
Caatinga	Experimental	FUNCEME	-6.7º	-40.3º	Air temperature Relative humidity Wind speed Precipitation Atmospheric pressure Solar radiation	29/12/2005 to 31/1/2018
	Headquarters of reserve	FUNCEME	-6.6º	-40.1º	Air temperature Relative humidity Wind speed Precipitation Atmospheric pressure Solar radiation	12/11/2005 to 10/1/2008
	Campos Sales	INMET	-7.1º	-40.4º	Air temperature Relative humidity Wind speed Precipitation Insolation Atmospheric pressure Solar radiation	1/11/1962 to 31/3/2019 8/3/2008 to 30/6/2019
	Tauá	INMET	-6.0º	-40.3º	Air temperature Relative humidity Wind speed Precipitation Insolation Atmospheric pressure Solar radiation	1/1/1964 to 3/8/2019 13/7/2007 to 30/6/2019
Pinares	Valladolid	AEMET	41.6º	-4.8º	Air temperature Relative humidity Wind speed Solar radiation Atmospheric pressure Precipitation	1/10/1973 to 13/10/2019 10/5/1991 to 30/9/2019 1/10/1973 to 14/10/2019
	Villanubla	AEMET	41.7º	-4.8º	Air temperature Relative humidity Wind speed	1/1/1961 to 13/10/2019

In the Caatinga forest, meteorological data were obtained from one of the four stations close to the area, depending on data availability on the analysis day (Figure 1): the Experimental station is located inside the experimental area and provided 27% of the data; the gauge located in the headquarters of the Ecological Station provided 8%; whereas Campos Sales and Tauá stations provided, respectively, 62% and 3% of the data. In the case of the Pinares forest, data concerning air temperature, wind speed and relative humidity were used from the Villanubla station, which is located outside the city of Valladolid and suffers less influence of urbanization effects. All other data were provided by the Valladolid station, which is closest to the area.

4.2.3 Surface Energy Balance Algorithm for Land (SEBAL) model

The Surface Energy Balance Algorithm for Land (SEBAL) model was applied in this work because it has been successfully used in this region and in several other investigations, whose objective was similar to ours. SEBAL calculates the components of the surface energy balance (LIAQAT; CHOI, 2015), so that the ET for each image pixel can be estimated using Eq. 1 (BASTIAANSSEN et al., 1998):

$$\lambda E_{inst} = R_N - G - H \quad (1)$$

where λE_{inst} is the latent heat flow at the time of imaging, R_N the net radiation on the surface, G the heat flow from the soil and H is the sensible heat flow. All units are W m^{-2}. R_N (Eq. 2) is a key hydrometeorological parameter and considers both short- and longwave radiation flows.

$$R_N = (1 - \alpha)R_{S\downarrow} + R_{L\downarrow} - R_{L\uparrow} - (1 - \varepsilon_S)R_{L\downarrow} \quad (2)$$

where α is the surface albedo and ε_S the surface emissivity, $R_{L\downarrow}$ and $R_{L\uparrow}$ are the respective surface upward and downward longwave radiations (W m^{-2}). $R_{S\downarrow}$ is the shortwave incoming radiation (W m^{-2}) and primary energy source for ET. The incoming shortwave radiation is obtained from Eq. 3:

$$R_{S\downarrow} = G_{SC}\, cos\theta\, dr\, \tau_{sw} \quad (3)$$

where G_{SC} is the solar constant (1367 Wm^{-2}), θ the solar incidence angle, dr the inverse squared relative distance between sun and earth, and τ_{sw} the atmospheric transmissivity, which can be calculated by the empirical Eq. 4.

$$\tau_{sw} = 0.75 + 0.00002z \quad (4)$$

where z is the height above mean sea level (m). The outgoing longwave $R_{L\uparrow}$ is obtained from Eq. 5:

$$R_{L\uparrow} = \varepsilon_0\, \sigma\, T_s^4 \quad (5)$$

where ε_0 is the (dimensionless) surface emissivity, σ the Stefan-Boltzmann constant (5.67×10^{-8} $Wm^{-2}K^{-4}$) and T_S the surface temperature (K). Emissivity can be calculated based on empirical equations of the Normalized Difference Vegetation Index (NDVI) and the leaf area index (LAI).

The leaf area index (Eq. 6) is calculated by using an empirical equation of the Soil Adjusted Vegetation Index (SAVI) (ALLEN et al., 2002):

$$LAI = -\frac{\ln\left(\frac{0.69 - SAVI}{0.59}\right)}{0.91} \quad (6)$$

SAVI (Eq. 7) is meant to reduce soil effect on reflectance of surface in arid areas and, thus, decreases soil moisture impacts on the index results (ALLEN et al., 2002).

$$SAVI = \frac{(R_{IR} - R_R)}{(L + R_{IR} + R_R)}(1 + L) \quad (7)$$

where R_{IR} and R_R are the reflectivity for infrared and red bands, respectively. L is a parameter for SAVI and if it is zero, SAVI becomes equal to NDVI. A value of 0.5 frequently appears in the literature for L and was used in this work. Incoming longwave radiation is calculated as in Eq. 8:

$$R_{L\downarrow} = \varepsilon_a \, \sigma \, T_a^4 \quad (8)$$

where ε_a is the atmospheric emissivity, and T_a the near surface air temperature (K). Soil and water heat flux G (Eq. 9) is the rate of heat storage in soil, plants and water in heat transfer. It is not possible to calculate this factor by remote sensing methods, but it can be determined relating G/R_n, NDVI, T_S and albedo.

$$\frac{G}{R_n} = \frac{T_S}{\alpha}(0.0038\alpha + 0.0074\alpha^2)(1 - 0.98NDVI^4) \quad (9)$$

where the surface temperature (T_S) is in °C. The sensible heat flux H (Eq. 10) is heat transferred to the air by convection due to a temperature difference.

$$H = \frac{\rho \, C_P \, \Delta T}{r_{ah}} \quad (10)$$

where ρ is air density, C_P the specific heat capacity of air for which 1004 $Jkg^{-1}k^{-1}$ was used, ΔT is the temperature difference from height Z_1 to Z_2 (K), and r_{ah} the aerodynamic resistance to heat transport ($s\ m^{-1}$). Since there are two unknown variables (ΔT and r_{ah}) in Eq. 10, acquiring a sensible heat flux can be complex. This is why the SEBAL process utilizes two "anchor" pixels, "hot" and "cold", to fix boundary conditions for the energy balance. The selected "cold" pixel is a wet, well-irrigated crop surface with full vegetation ground cover. The surface and

near-surface air temperatures are assumed to be equal at this pixel. The selected "hot" pixel is a dry, bare agricultural field with ET assumed to be zero (ALLEN et al., 2002).

Two factors must be taken into account when choosing "anchor" pixels: surface temperature (T_S) and vegetation index (NDVI). The cold pixel must have a low temperature and a high NDVI, whereas the hot pixel must have a high temperature and a low NDVI (RAHIMZADEGAN; JANANI, 2019). A linear relationship is established between T_S and ΔT Eq. 11 and calibrated based on the knowledge of the boundary conditions identified in the "anchors", where the ΔT values can be calculated back using a known H.

$$\Delta T = b + aT_S \tag{11}$$

In Eq. 11, 'a' and 'b' are parameters. The variables ΔT and r_{ah} are calculated in the first loop, subsequently current values are implemented in the next loop as new initial values, and variables are updated in every loop. This process continues until the variables converge, which enables the algorithm to assess the sensible heat flux (LOSGEDARAGH; RAHIMZADEGAN, 2018).

The SEBAL model was applied in GRASS GIS 7.6, the Geographic Information System called Geographic Resources Analysis Support System; a script developed for each Landsat platform was used to facilitate the loop procedure to obtain ΔT, r_{ah} and, consequently, H.

The instantaneous ET value (mm h^{-1}) at the time of image acquisition and in an equivalent evaporation depth is computed as in Eq. 12:

$$ET_{inst} = 3600\frac{\lambda E_{inst}}{\lambda} \tag{12}$$

where 3600 is the time conversion from seconds to hours, and λ the latent vaporization heat or the heat absorbed when a kilogram of water evaporates (J kg^{-1}). After this, the daily ET value (mm day^{-1}) can be computed as in Eq. 13:

$$ET_{day} = \frac{ET_{inst}}{ET_r} ET_{r_{day}} \tag{13}$$

where ET_r is the reference ET at the time of the image. For natural forest areas, ET_{inst}/ET_r, denominated evapotranspiration faction (ET_{frac}), is similar to the product between crop coefficient (K_c, dimensionless) and water stress coefficient (K_s, dimensionless). $ET_{r_{day}}$ is the cumulative 24-hour ET_r for the day of the image. Both ET_r and $ET_{r_{day}}$ were obtained with the program REF-ET 4.1 (ALLEN, 2016) (mm h^{-1}) by using the Penman-Monteith FAO equation

(PM-FAO: Allen, Pereira, Raes, & Smith, 1998). The actual annual evapotranspiration to be used in trend analyses was derived from ET_{frac} data.

Figure 4 - Flowchart of actually daily ET estimation by using Landsat images and SEBAL model

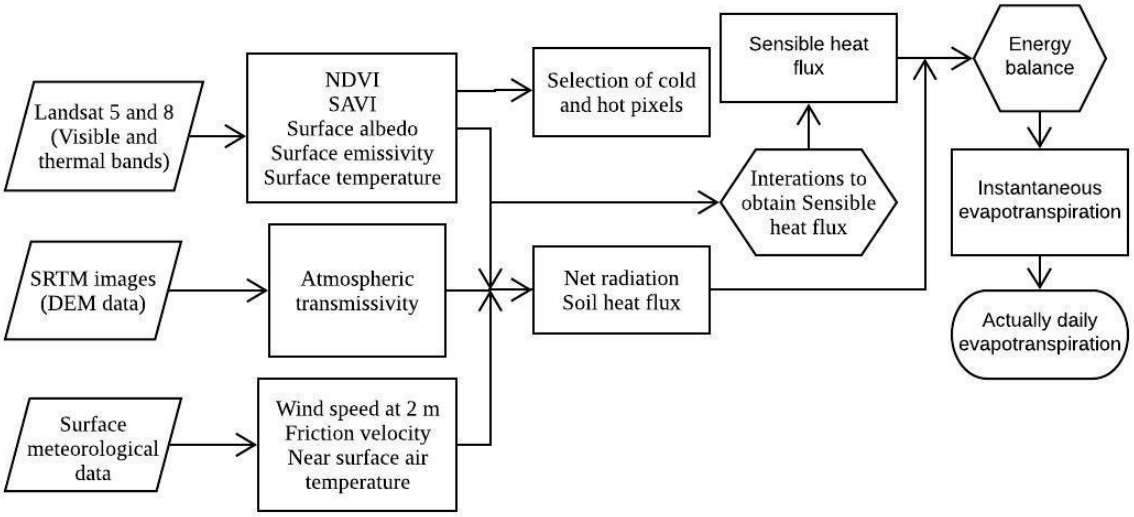

4.2.4 Comparison of ET_a by SEBAL with FAO56 Method and climate change trend analysis

In order to compare the results obtained through SEBAL with another method we used the Eq.14.

$$ET_a = ET_0.K_c.K_s \tag{14}$$

For both semiarid zones the ET_0 was determined by using Penman-Monteith FAO56 equation (ALLEN et al., 1998).Three statistical metrics were used: the determination coefficient (R^2, Eq.15), Nash–Sutcliffe efficiency coefficient (NSE, Eq.16), and Pearson's correlation coefficient (r, Eq.17).

$$R^2 = \frac{\left[\sum_{i=1}^{n}(ETa_{Sebal,i} - \overline{ETa}_{Sebal})(ETa_i - \overline{ETa})\right]^2}{\sum_{i=1}^{n}(ETa_{Sebal,i} - \overline{ETa}_{Sebal})^2 \sum_{i=1}^{n}(ETa_i - \overline{ETa})^2} \tag{15}$$

$$NSE = 1 - \frac{\sum_{i=1}^{n}(ETa_i - ETa_{Sebal,i})^2}{\sum_{i=1}^{n}(ETa_i - \overline{ETa}_i)^2} \tag{16}$$

$$r = \frac{\sum_{i=1}^{n}(ETa_{Sebal,i} - \overline{ETa}_{Sebal})(ETa_i - \overline{ETa})}{\sqrt{\sum_{i=1}^{n}(ETa_{Sebal,i} - \overline{ETa}_{Sebal})^2 \sum_{i=1}^{n}(ETa_i - \overline{ETa})^2}} \tag{17}$$

where $ETa_{Sebal,i}$ is the SEBAL actual evapotranspiration for each day and ETa_i the actual evapotranspiration obtained by Eq. 14.

The trend analysis was performed using Mann-Kendall method (KENDALL, 1975; MANN, 1945): it is a nonparametric test to identify a trend in a series. The null hypothesis H_0 for this test means that there is no trend in the series, whereas the three alternative hypotheses are a negative, non-null, or positive trend. A significance level of p = 0.05 was applied in this study. The Mann-Kendall test was employed with weather variables (rainfall, maximum and minimum temperature) and with the actual and potential evapotranspiration.

4.2.6 Temporal Stability Index

The Temporal Stability Index (TSI) was calculated as in Penna et al. (2013) and in Zhao et al. (2010) for each season (autumn, winter, spring and summer) in the Pinares forest. For the Caatinga forest, we calculated TSI for the rainy season and for the dry season, since the four seasons cannot be differentiated there. Eqs. 17, 18, and 19 were used to assess the TSI:

$$\delta_{ij} = \frac{(ETa_{ij} - \overline{ETa_j})}{\overline{ETa_j}} \tag{17}$$

$$\sigma_{ij} = \sqrt{\frac{(ETa_{ij} - \overline{ETa_j})^2}{np - 1}} \tag{18}$$

$$\text{TSI} = \sqrt{{\delta_{ij}}^2 + \sigma_{ij}{\delta_{ij}}^2} \tag{19}$$

where ETa_{ij} is the actual evapotranspiration value at position i at time j, $\overline{ETa_j}$ the average actual evapotranspiration of all positions in space at time j, σ the standard deviation and np the number of pixels. Low TSI values indicate zones with high temporal stability of ET_a, while high TSI values indicate zones of low stability over time.

4.3 Results and Discussion

4.3.1 Time series analysis of evapotranspiration

Figure 5 shows the daily time series of potential and actual evapotranspiration, as well as precipitation. It can be seen that the daily amplitude of ET_0 in both areas is similar: they range from 2 to 10 mm day^{-1} in the Caatinga forest and from 0 to 8 mm day^{-1} in the Pinares forest. In the Caatinga forest, however, there is a greater daily variability, since the area does not have a well-defined distinction between the four seasons (winter, spring, summer, autumn). We also observe that ET_a is much closer to ET_0 in the Pinares forest, especially in the winter (December-February), when the atmospheric water demand is lower. In summer (June-August), the soil is drier due to the combination of high potential evapotranspiration and low precipitation (CALAMA et al., 2019), which diminishes soil moisture and, consequently, actual evapotranspiration.

Figure 5 - Time series of daily rainfall and actual (ET_a) and potential evapotranspiration (ET_0) for (a) the Caatinga forest and (b) the Pinares forest. Daily values are interpolated from the satellite overpass time

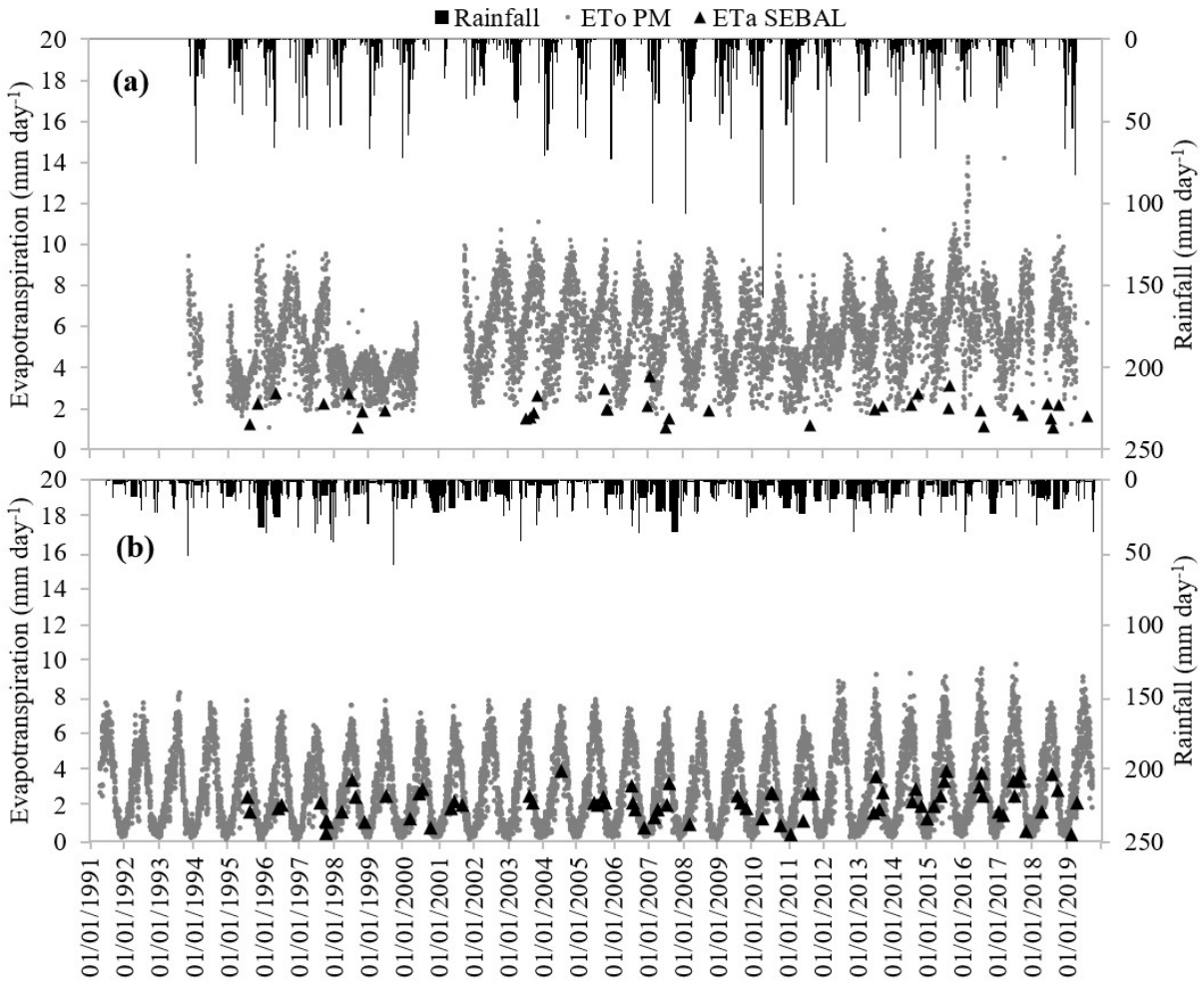

During the dry season in the Caatinga forest, actual evapotranspiration is generally much lower than the potential one (Figure 5a). In that period, the potential evapotranspiration is high due to high air temperature and low air moisture, which raise the vegetative water demand. Simultaneously, water availability for the plants is limited due to a continuous absence of precipitation for several months (MEDEIROS; DE ARAÚJO, 2014), so that soil moisture is extremely low (in the Caatinga forest, moisture is below wilting point during more than six months annually: Costa, Lopes, Pinheiro, Araújo, & Gomes Filho, 2013). The combination of high atmospheric-water demand and low soil-water availability causes the plants to actually evapotranspirate considerably less than the potential value. During the rainy season (January-April) (Figure 2a), in contrast, soil moisture increases and potential evapotranspiration decreases (Figure 5b).

Due to the presence of clouds, it was not possible to obtain images during the rainiest months of the year (February, March and April in the Caatinga forest and December in Pinares). According to Jaafar and Ahmad (2020), some limitation exists when cloudy days are frequent: estimated ET_a may be higher than the actual values during winter and early spring, considering that the cloudless images are not representative of that period, and in images of cloudy days, evapotranspiration is below the period average. This is true for the Brazilian semiarid during the rainy season, when cloudiness prevails, and it explains why the curve generated in Figure 6a is incomplete. Despite data gaps, however, one can observe the annual behaviour of Kc.Ks in both areas and its value can be used for prospective estimates of ET_a. According to Teixeira et al. (2009), the value of Kc.Ks during the Caatinga dry season is around 0.20. For the present study, the maximum Kc.Ks value could not be identified, considering that no useful images were available during the months with the highest precipitation rates. In accordance with the authors *op cit.*, the Kc.Ks may surpass 0.90 during wet season in a Caatinga vegetation. This value was admitted for the months of February, March and April for the complete construction of Figure 6c.

Figure 6 - Monthly fraction of evapotranspiration ($ET_{frac} = K_c.K_s$) for both forests (a) Caatinga and (b) Pinares obtained by ET_{a_SEBAL}/ET_{0_PM} for each scene of Landsat used and (c) for each month by ET_{frac} average

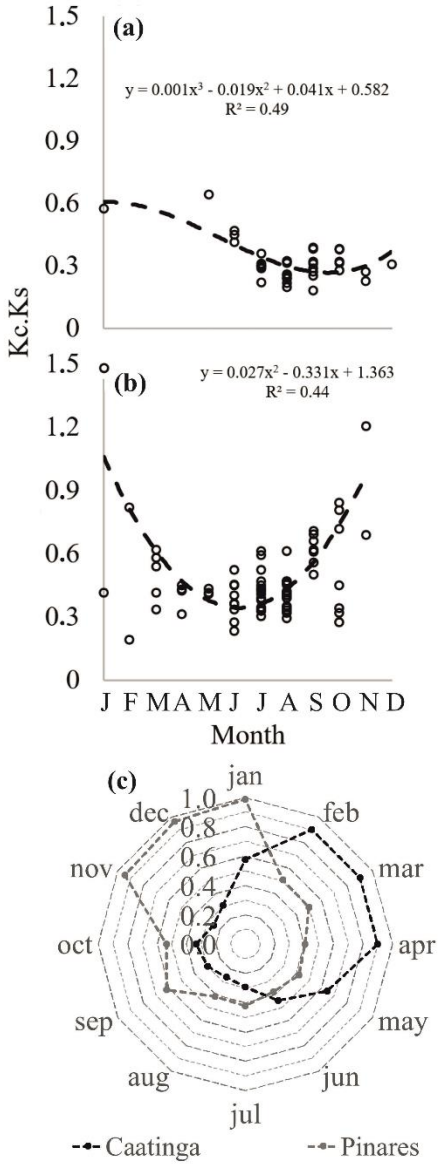

With regards to the Pinares forest (Figure 6b), a large dispersion of Kc.Ks data in late autumn and winter can be perceived; it may be related to the high daily ranges of wind speed (standard deviation = 1.9 m s^{-1}) and precipitation (standard deviation = 3.9 mm) during that period. The gradient of water potential in the soil-plant-atmosphere complex causes soil water to be carried through the plant and transpired through the leaves. When the precipitation rate is low and there is not enough soil moisture present, the water potential gradient is reduced and does not favour transpiration. Wind also influences the evapotranspiration process, as it carries moist air over the surface of leaves, soil and water bodies, renewing the air and keeping

it prone to receive more steam. Thus, the daily variation of these factors influences the increase and decrease of ET_a and it explains the dispersion of Kc.Ks in the Pinares forest.

The box-plot of the daily actual evapotranspiration in Figure 7 is divided into colours corresponding to the seasons for the two study areas. As in the Brazilian semiarid zone the four typical seasons are not well-defined like in the Pinares forest, only rainy (first semester) and dry seasons (second semester) are distinguished. The individual box-plots correspond to the ET_a data of each of the pixels of the images that represent the two studied sites. There is a greater amplitude in the Caatinga forest ET_a data (Figure 7a) than in the Pinares forest (Figure 7b), with statistical significance at the 95% confidence level by the ANOVA F test.

Figure 7 - Box-plot of daily actual evapotranspiration (ET_a) for the two forests (a) Caatinga (N ≈ 146,799 pixels) and (b) Pinares (N ≈ 168,956 pixels), elaborated for each of 111 Landsat overpasses and computed by using the Surface Energy Balance Algorithm for Land (SEBAL) model. The colours represent the different seasons of the year

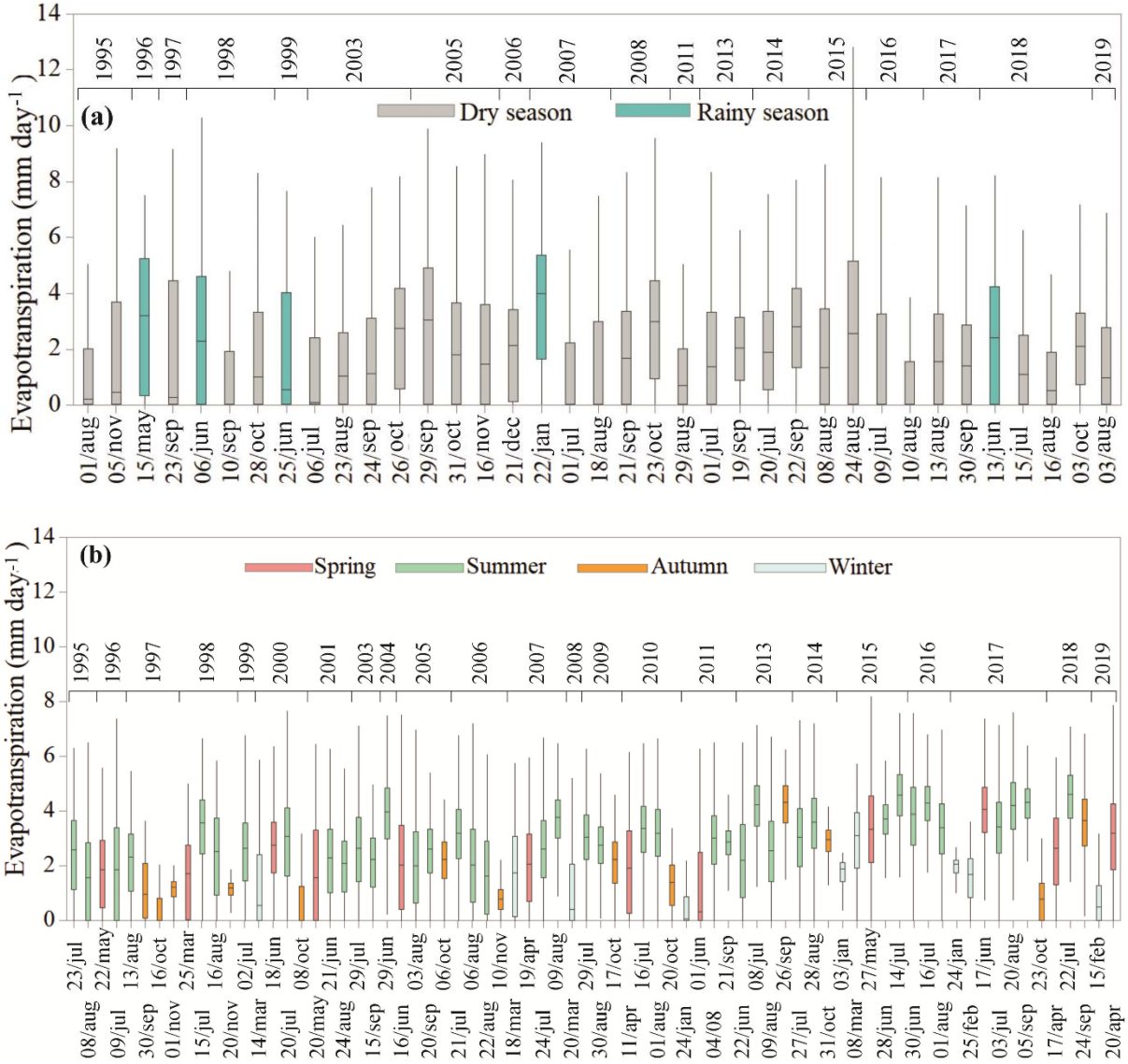

The Caatinga forest is an area of natural vegetation and, hence, characterized by a wider range of species and a higher irregularity in the distribution of vegetation density, if compared to the Pinares forest. It may also be highlighted that there are pixels of reservoir water or rivers and pixels of exposed soil from roads and badlands in both areas; these pixels influence the respective maximum and minimum ET_a peaks. Many pixels in the Caatinga area show a value of ET_a equal or close to zero in almost all the images due to exposed soil areas and/or the presence of leafless plants that, according to the method, resemble exposed soil. In some cases, such as on 10/Sep/1998, 1/Jul//2007, 18/Aug/2007, 9/Jul/2016, 10/Aug/2016 the median was

zero; note that the first and last of these three years (1998 and 2016) were very dry (see Figure 5a). In the Pinares forest the medians are higher in Summer and Spring, whereas Autumn and Winter have the lowest atmospheric demands of the year.

As there is no agricultural production around the study areas during some months, such as in the dry season at Caatinga forest and winter at the Pinares forest, it was difficult to choose a cold pixel for the execution of SEBAL; that being so, a pixel within a water body was selected. This circumstance makes it a somewhat inconvenient method to be used in natural areas. Still, the ET_a data obtained using SEBAL adjust well to the ET_a data assessed by Penman-Monteith times Kc and Ks (Figure 8a, b). In the Pinares forest, we used the seasonal value of the ratio ET_a/ET_0 (it means Kc.Ks) obtained by Liu et al. (2017) for pines using eddy flux (FLUXNET) data (Table 2). In the Caatinga forest (Table 2), ET_a/ET_0 was calculated from the on-site water balance by Teixeira (2018). Teixeira et al. (2009) also found a good correlation ($R^2 = 0.87$) between the daily ET_a data by SEBAL and field data from a mixed agricultural and natural ecosystem in a Brazilian semiarid region.

Figure 8 - Validation of daily actual evapotranspiration (ET_a) for the two forests: (a) Caatinga and (b) Pinares, using ET_0 calculated with the Penman-Monteith FAO-56 equation and $K_c.K_s$

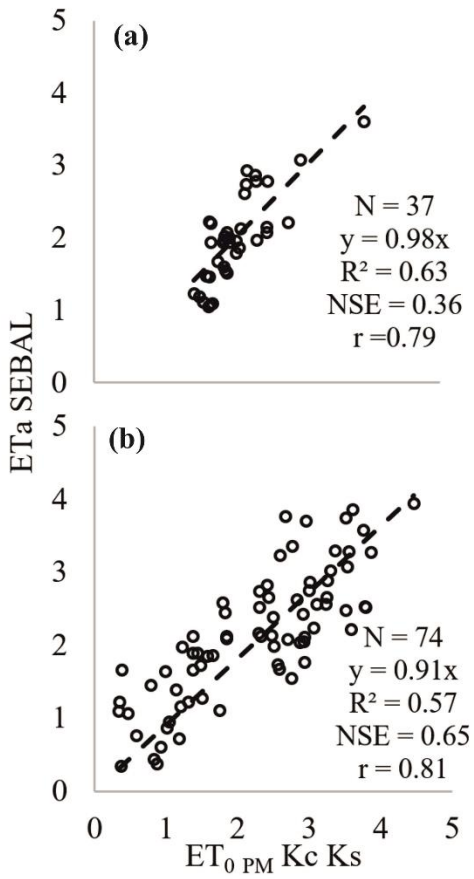

The statistical parameters are determination coefficient (R^2), Nash–Sutcliffe coefficient (NSE), and Pearson's correlation coefficient (r).

Table 2 - Ratio ET_a/ET_0 (which equals $K_c.K_s$, Eq. 13) for the Caatinga (TEIXEIRA, 2018) and Pinares (Liu et al., 2017) semiarid forests

Area	Months											
	J	F	M	A	M	J	J	A	S	O	N	D
Caatinga	0.62	0.76	0.68	0.81	0.54	0.36	0.34	0.30	0.29	0.31	0.29	0.37
Pinares	0.44	0.44	0.37	0.37	0.37	0.49	0.49	0.49	0.52	0.52	0.52	0.44

In both forests, the correlation between NDVI and ET_a was greater in areas of less dense vegetation (Figure 9). As the most vegetated areas have a more constant NDVI throughout the year, the annual variations of ET_a are more dependent on meteorological factors (related to the atmospheric demand for humidity) than on vegetation. Areas of less dense vegetation, on the other hand, show greater variation in NDVI according to the season. In the case of the Caatinga forest, NDVI is highly influenced by the variation of soil moisture between the rainy and dry months, and in the Pinares vegetation the NDVI varies depending on the four seasons of the year. It is also possible to observe greater NDVI ET_a correlations in the Caatinga than in Pinares. This is due to the strong deciduousness that exists in Caatinga vegetation in the dry months, causing the NDVI to vary more throughout the year.

Figure 9 - Pearson's correlation (r) between Normalized Difference Vegetation Index (NDVI) and actual evapotranspiration (ET_a) for each pixel of Caatiga forest (a) and Pinares forest (b) images

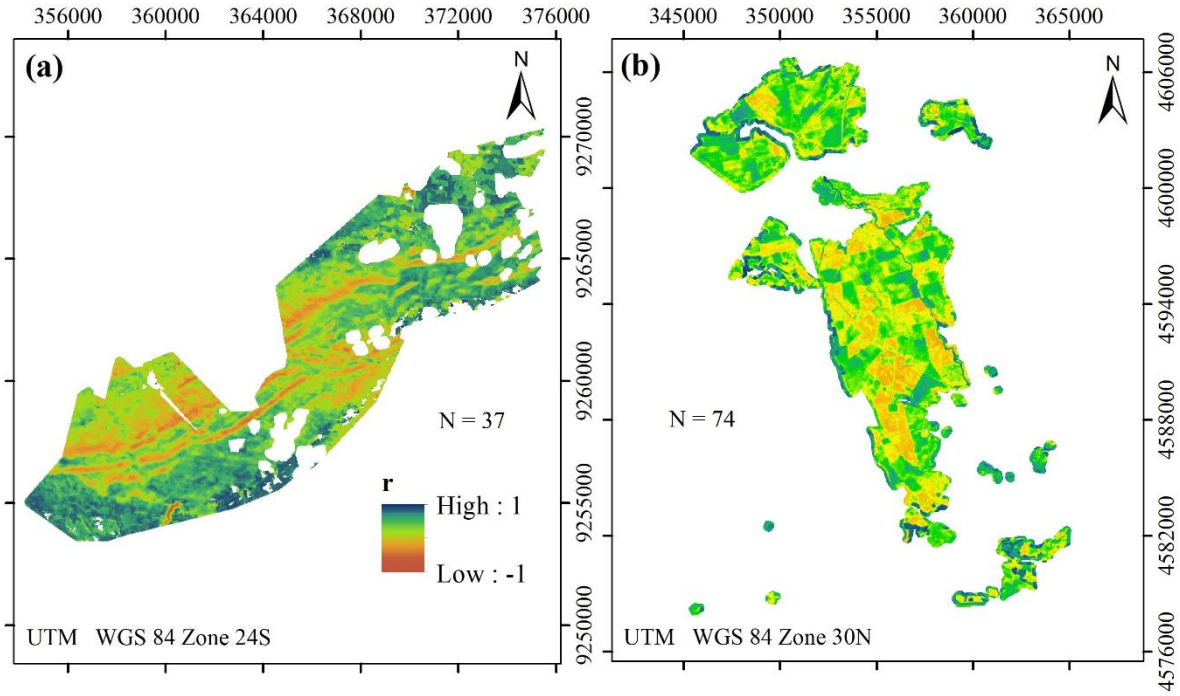

4.3.2 Temporal Stability Index (TSI) of actual ET

In Figure 10 it may be noticed that the zones of lower and higher TSI are always the same in both areas; what changes from season to season is the intensity. The areas with the highest TSI are the ones that respond strongest to differences in soil moisture. In the Caatinga forest, these are the highest regions with denser vegetation and, consequently, a high capacity to expand leaf mass and increase evapotranspiration when soil moisture is higher after a precipitation event. High TSI values can also be observed in areas of exposed soil at the edges of the study area. There herbaceous vegetation grows during the rainy season, disappears during the dry season and leaves the soil bare. According to Tasumi (2019), in bare soils, ET is often overestimated, since there the ET_a in dry seasons should be near zero. The overestimated amount is not negligible when compared to annual precipitation.

Figure 10 - Temporal Stability Index (TSI) of ET_a for the (a) rainy season and (b) dry season of the Caatinga forest, and for the four seasons (c) spring, (d) summer, (e) autumn and (f) winter of the Pinares forest

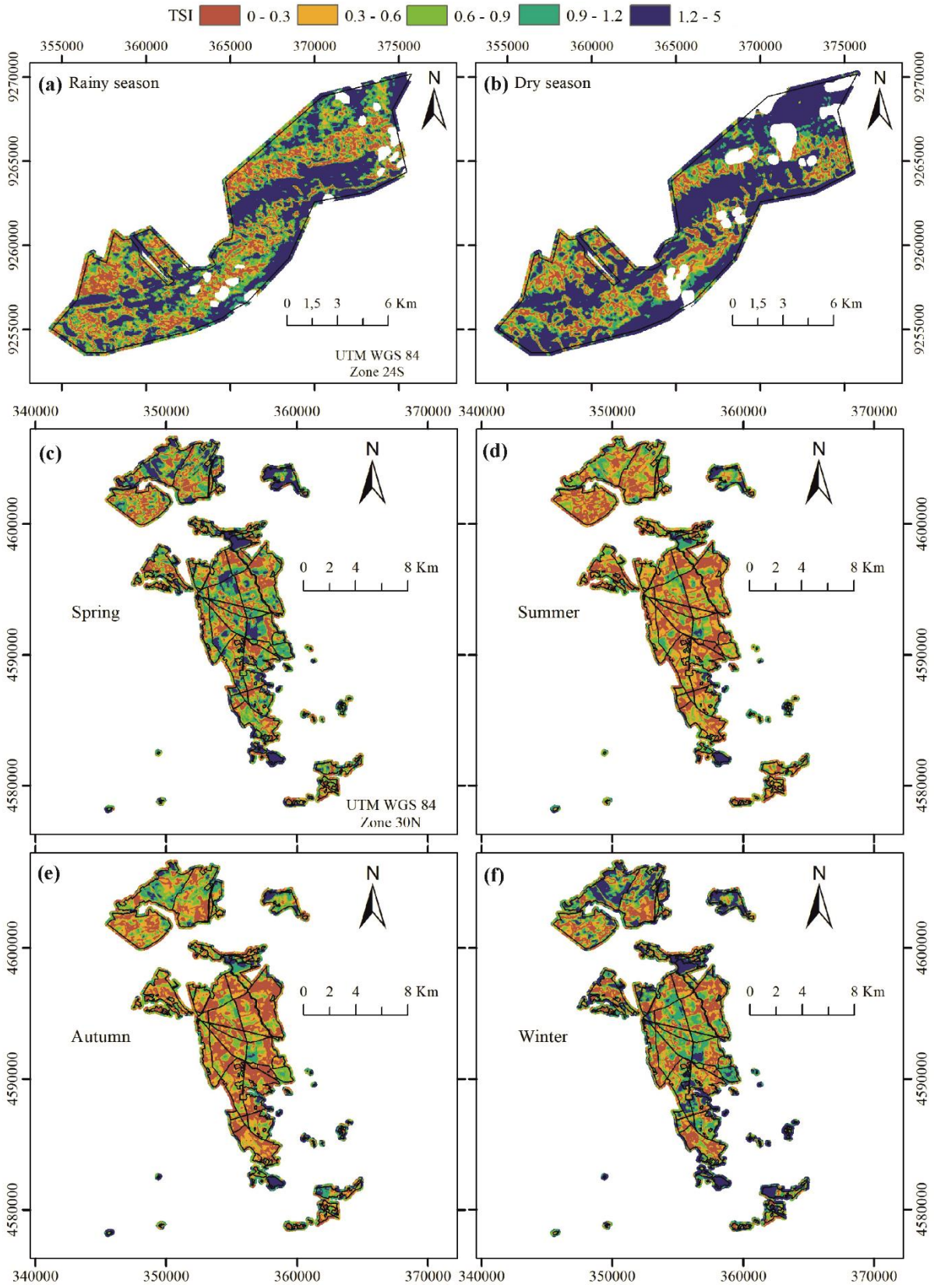

The same observations in relation to exposed soil areas can be made in the Pinares forest, especially during winter and spring. There, however, unlike in the Caatinga forest, the areas with the highest TSI have sparse vegetation, as they produce a more substantial herbaceous layer under proper environmental conditions.

The Caatinga forest presents a greater extension with lower temporal stability than the Pinares forest (Figure 10). This is due to the greater variety of species in the Caatinga with different transpiration strategies and growth stages throughout the year, as well as to the fact that vegetation density throughout the area demonstrates a greater variation.

4.3.3 Climate change and trends in evapotranspiration (ET)

Evapotranspiration is a very complex process and influenced by many factors as precipitation, temperature, radiation, wind speed (YANG et al., 2019), type and stage of vegetation. That is why it is important to identify eventual existing trends in variables that influence ET_a trend interpretations (JAAFAR; AHMAD, 2020). In order to investigate the reasons for ET_a changes, three basic factors that control ET were calculated for the study period (Figure 11 and Table 3): ET_0 and temperature indicate the atmospheric demand; whereas precipitation, which is an indicator of water availability for evapotranspiration. According to Yang et al. (2019), surface moisture, which is affected by precipitation, is the basic material for the ET_a process and also the main limiting factor in arid and semiarid regions.

Figure 11 - Yearly data of the variables used for trend analysis ((a, d) rainfall; (b, e) maximum and minimum temperature; and (c, f) potential and actual evapotranspiration, ET_0 and ET_a, respectively) for (a, b, c) Caatinga forest and (d, e, f) Pinares forest. Yearly ET_a was calculated by multiplying monthly ET_{frac} (K_c.K_s) and daily Penman-Monteith ET_0

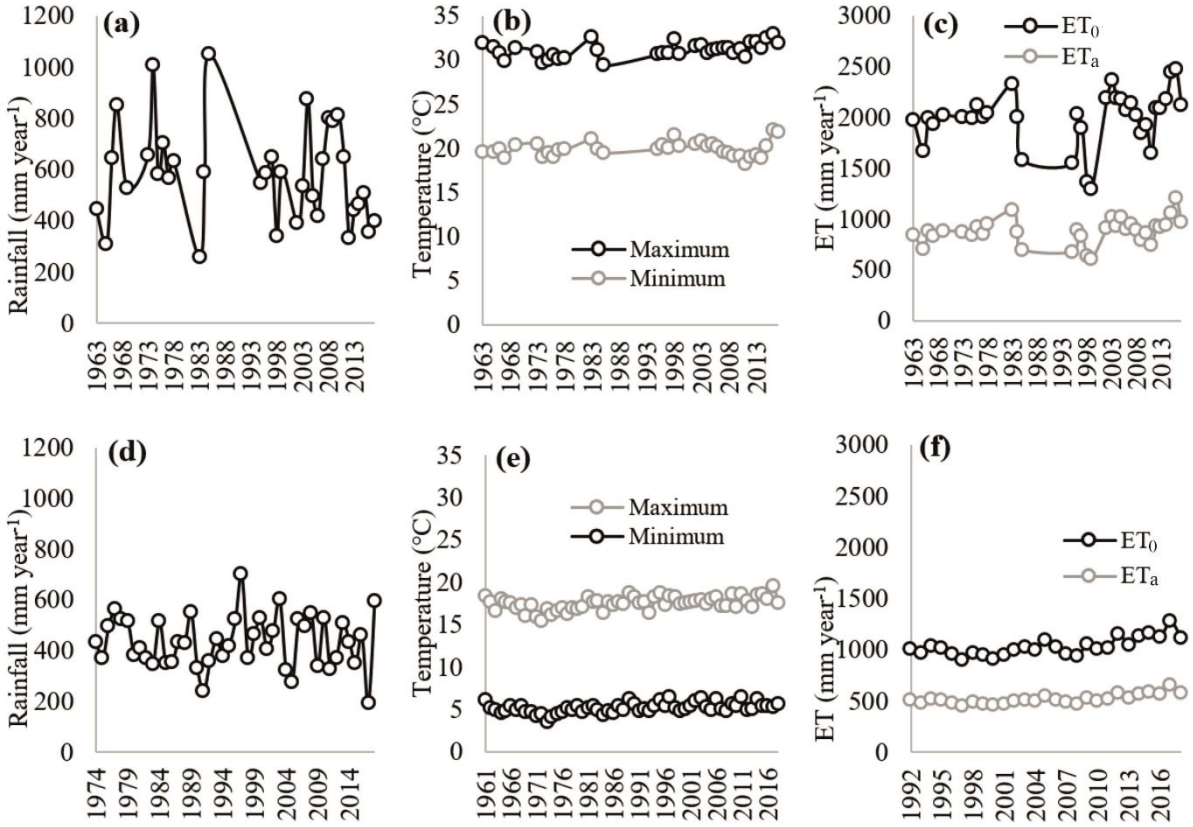

Table 3 - Trend analysis of weather variables and potential and actual evapotranspiration (ET_0 and ET_a, respectively). S indicates the trend (negative or positive), Sen's Slope represents the annual increase/decrease of the variable and p-value is the trend significance. *There is a significant positive temporal trend at the 5% level

	Variable	years	Mean	τ	S	Slope	p-value
Caatinga	Rainfall (mm year^{-1})	35	582.880	-0.133	-79.000	-2.427	0.268
	Maximum temperature (°C)	35	31.066	0.324	193.000	0.027	0.003*
	Minimum temperature (°C)	35	19.878	0.052	31.000	0.005	0.670
	ET_0 (mm year^{-1})	34	1989.845	0.262	147.000	3.546	0.015*
	ET_a (mm year^{-1})	34	876.795	0.273	153.000	2.170	0.012*
Pinares	Rainfall (mm year^{-1})	45	434.056	-0.002	-2.000	-0.065	0.992
	Maximum temperature (°C)	58	17.473	0.315	521.000	0.023	0.000*
	Minimum temperature (°C)	58	5.132	0.308	509.000	0.014	0.000*
	ET_0 (mm year^{-1})	27	1025.388	0.470	165.000	7.084	0.000*
	ET_a (mm year^{-1})	27	513.400	0.493	173.000	3.925	0.000*

When no monthly value of Kc.Ks produced by SEBAL was available, values from literature were used to calculate the ET_a. In the Caatinga area, maximum temperature, annual Penman-Monteith ET_0 and annual ET_a present a discernible positive trend over the period 1963–2017. Annual maximum air temperature increased at 0.027 °C per year (which means in arithmetic progression 1.5 °C over 55 years). During the study period, in the Caatinga, neither annual rainfall (mean 583 mm yr^{-1}) or minimum temperature (mean 20 °C) trends were statistically significant (Table 3). The ET_0 displays a mean value of 5.5 mm d^{-1} (total of 1990 mm yr^{-1}), a minimum of 1298 mm (during the year of 1999, Figure 11a), a maximum of 2466 mm (in the dry and hot year of 2016, Figure 11 a, b) and an increase of 3.5 mm yr^{-1}, which means that it rose by 192.5 mm during the analysed period. ET_a showed a significant positive trend with annual increase of 2.2 mm (121 mm over the investigated time span).

In the Pinares forest precipitation has a non-significant negative trend, while all the other analysed variables showed a significant positive temporal trend. The maximum temperature (17.5 °C) showed a trend of 0.023 °C per year, which supports the results of del Río, Fraile, Herrero, and Penas (2007) who worked with a historical series (1961–1997) for the Castile and Leon region and assessed a trend of 0.02 °C yr^{-1} and the results of Moratiel, Snyder, Durán, and Tarquis (2011), for the Duero Valley (historical series of 1980–2009), who found a trend of 0.03 °C yr^{-1} for the period. The minimum temperature (5 °C) of the Pinares forest showed a trend of 0.014 °C per year; again, del Río, Fraile, Herrero, and Penas (2007) computed a very similar result for the same variable: a temporal trend of 0.01 °C yr^{-1} for the minimum temperature in Castile and Leon. ET_0 showed a trend of 7.0 mm yr^{-1} (191 mm for all the period), higher than the trend of 10 mm $decade^{-1}$ found by Vicente-Serrano et al. (2014). The mentioned authors used a larger time series for their study (1961-2011). They found a more linear ET_0 pattern until 1990, after that period, coinciding with the years of our historical series, ET_a had a greater annual increase. That means that we find a greater tendency for an annual increase in ET_a due to the size of the historical series studied (1992-2018). In the series established for the present study, the minimum ET_0 was 897 mm (during the wet year of 1997, the rainiest in the series, Figure 11d), and the maximum value was 1278 mm in 2017 (the year with the highest maximum temperature, Figure 11e). Likewise, the ET_a (average 513.4 mm yr^{-1}) presented an increasing trend of 3.9 mm yr^{-1} (106 mm for the period), so that the ET_a variation was also similar to ET_0 throughout the period (Figure 11f).

In both study areas, the annual ET_a was assessed to be superior to annual precipitation. The Pinares pine stone forest benefits from the moisture of the water table of the

Pisuerga, Duero, Cega and Adaja rivers. In the Caatinga forest, the explanation may stem from the fact that part of a reservoir, named Benguê, is within this area and it receives input from a larger area (932 km^2). Thus, the reservoir evaporation and the maintenance of a higher humidity in the surrounding soil could justify an annual ET_a greater than precipitation in the area.

It is interesting to observe that annual ET_0 and ET_a in Caatinga Forest (10° South latitude) are almost twice than in Pinares forest (40° North latitude). This is an important result that must be studied in other semiarid environments with different latitudes.

In order to know whether the historical data series show dependency, we performed an autocorrelation analysis, using precipitation and (actual and potential) evapotranspiration data. The results indicate that no autocorrelation was found in Caatinga or in Pinares for 5% significance. However, both series of evapotranspiration presented statistically significant first-order autocorrelation (Lag 1): 50% both in Caatinga and Pinares. This means that, for half of the year, the evapotranspiration depends on that of the previous year.

Although annual ET_a is higher in the Caatinga than in Pinares, the observed temporal increasing rate of evapotranspiration in the Spanish site prevails. Using the rates estimated in this research, the Spanish region would have an equivalent ET_a of the present-day Caatinga by the end of the XXI Century (within approximately 70 to 100 years). This extrapolation is engendered with uncertainty, however, the increasing trend of the evapotranspiration in the Pinares should be taken seriously, and the Caatinga can be taken as a significant hydrological mirror.

Yang et al. (2019) studied the semiarid zones of South America and also identified increasing trend for potential evapotranspiration. However, the authors *op cit.* estimated a decrease in actual evapotranspiration of 3.5 $mm.yr^{-1}$. The reason for this trend would be the reduction of soil water, which implies that water availability is the limiting fator to ET_a. According Marengo et al. (2020), until 2100, it is expected an increase of up to two months per year in the dry season in the Brazilian Northeastern region. This change may cause a significant decrease in the natural vegetation. Besides, the natural vegetation can stay longer without the leaves, which also contributes to the decrease of actual transpiration. Contrastingly, the increment of ET_a in the Spanish area can be caused mainly by the rise of the potential evaporation, considering that there the water availability is remarkably higher than in the Brazilian site.

This trend is an indication that Spanish decision makers should analyze other semiarid environments in the globe so as to adapt to the consequences for biodiversity and water availability, not only in the soil, but also in the reservoirs. Among possible consequences, there

is the reduction of regenerative capacity of vegetation, particularly Pinus *pinaster* (VERGARECHEA et al., 2019).

4.4 Conclusions

We noticed in our work that ET_a in denser vegetation areas is more dependent on meteorological factors (related to atmospheric demand for humidity) than on vegetation. This behaviour is common to both forests. The irregular distribution of vegetation density, the presence of reservoir water or rivers and pixels of exposed soil from roads and badlands influenced the values of maximum and minimum ET_a.

The Caatinga forest showed greater spatial variation of ET_a than the Pinares forest. The zones of a lower and higher Temporal Stability Index (TSI) of ET_a are always the same in both areas throughout the year, what changes from season to season is the intensity. The areas with the highest TSI are those that respond most to differences in soil moisture. In the Caatinga forest these are the highest areas of denser vegetation with their huge capacity to expand leaf mass and increase evapotranspiration, when soil moisture rises after precipitation. The Caatinga forest presents a greater extension with lower temporal stability than the Pinares forest.

The results of this work indicate that the actual evapotranspiration of the Spanish Pinares zone is increasing more rapidly than in the Caatinga, which can serve as a hydrological mirror to the Spanish site. If this trend is confirmed, significant change in soil and reservoirs water balance is expected. In the Caatinga, the water availability is the limiting factor to the evolution of the actual evapotranspiration. Contrastingly, in Pinares, the evolution of the actual evapotranspiration is more severely affected by the augmentation of the potential evapotranspiration, considering the higher water availability in the soil.

Studies like ours could be applied to other similar areas around the world, and to other hydrological processes, using one area as a reference, a possible hydrological mirror for the other.

5 FINAL CONSIDERATIONS

Through this PhD Thesis it was possible to answer the guiding questions presented in the introduction. With this, we add to the state-of-the-art important scientific information about the water dynamics in the soil-plant-atmosphere continuum. We identified the points of humidity in the stem capable of stimulating the emergence of the first leaves in the rainy season. We observed in this study the comparative importance of water stored in plants compared to water stored in surface reservoirs. We saw the ability of the species studied to perform reverse sap flow. We established the concept of a hydrological mirror between distinct forest areas and identified trends for increased evapotranspiration in semi-arid forests.

REFERENCES

ALLEN, R. et al. **SEBAL, Surface Energy Balance Algorithms for Land. Idaho Implementation - Advanced Training and Users Manual**. Idaho: [*s.n.*], 2002.

ALLEN, R. G. et al. **Crop Evapotranspiration: guidelines for computing crop water requirements**. FAO Irrigation and drainage paper 56. Food and Agriculture Organization, Rome: [*s.n.*], 1998.

ALLEN, R. G. **REF-ET: Reference evapotranspiration calculator.** Idaho: University of Idaho, 2016.

ALVES JUNIOR, F. T. **Estrutura, biomassa e volumetria de área de Caatinga, Floresta-PE**. 2010. 123 f. Dissertation (Doutorado em Ciências Florestais), Departamento de Ciência Florestal, Universidade Federal Rural de Pernambuco, Recife, 2010.

AMARAL, A. M. et al. Uncertainty in sap flow of Brazilian mahogany determined by the heat ratio method. **Journal of Forestry Research**, [*s.l.*], v. 1, 2020.

ARAÚJO, E. M. **Estimativa do assoreamento de um pequeno reservatório do semiárido rural através do estudo dos solos e de fontes de sedimento.** 2013. 87 f. Thesis (Mestrado em Engenharia Agrícola) - Programa de Pós-Graduação em Engenharia Agrícola Universidade Federal do Ceará, Fortaleza-CE, 2012.

ARAÚJO, G. P. et al. A low-cost monitoring system of stem water content: Development and application to Brazilian forest species. **Smart Agricultural Technology**, [*s.l.*], v. 1, 1 dez. 2021.

BASTIAANSSEN, W. G. M. et al. A remote sensing surface energy balance algorithm for land (SEBAL): 1. Formulation. **Journal of Hydrology**, [*s.l.*], v. 212–213, n. 1–4, p. 198–212, 1998.

BELLO, J. A. L. El Pinar de Antequera (Valladolid, España): flora vascular de interés. **Botanica Complutensis**, [*s.l.*], v. 28, p. 67–70, 2004.

BERRY, Z. C.; WHITE, J. C.; SMITH, W. K. Foliar uptake, carbon fluxes and water status are affected by the timing of daily fog in saplings from a threatened cloud forest. **Tree Physiology**, [*s.l.*], v. 34, n. 5, p. 459–470, 2014.

BORCHERT, R. Soil and stem water storage determine phenology and distribution of tropical dry forest trees. **Ecology**, [*s.l.*], v. 75, n. 5, p. 1437–1449, 1994.

BORETTI, A.; ROSA, L. Reassessing the projections of the World Water Development Report. **npj Clean Water**, [*s.l.*], v. 15, p. 1–6, 2019.

BURGESS, S. S. O. et al. An improved heat pulse method to measure low and resever rates of

sap flow in woody plants. **Tree Physiology**, [*s.l.*], v. 21, p. 589–598, 2001.

BURGESS, S. S. O.; DAWSON, T. E. The contribution of fog to the water relations of Sequoia sempervirens (D. Don): foliar uptake and prevention of dehydration. **Plant, Cell and Environment**, [*s.l.*], v. 27, n. 8, p. 1023–1034, 2004.

BURKHARDT, J. Hygroscopic particles on leaves: nutrients or desiccants? **Ecological Monographs**, [*s.l.*], v. 80, n. 3, p. 369–399, 2010.

BURKHARDT, J. et al. Stomatal penetration by aqueous solutions - an update involving leaf surface particles. **New Phytologist**, [*s.l.*], v. 196, n. 3, p. 774–787, 2012.

CALAMA, R. et al. Linking climate, annual growth and competition in a Mediterranean forest: Pinus pinea in the Spanish Northern Plateau. **Agricultural and Forest Meteorology journal**, [*s.l.*], v. 264, p. 309–321, 2019.

CARRASCO, L. O. et al. Water storage dynamics in the main stem of subtropical tree species differing in wood density, growth rate and life history traits. **Tree Physiology**, [*s.l.*], v. 35, p. 354–365, 2014.

CARRILLO-LÓPEZ, A.; YAHIA, E. M. Morphology and Anatomy. **Postharvest Physiology and Biochemistry of Fruits and Vegetables**, p. 113–130, 2019.

CASSANA, F. F. et al. Effects of soil water availability on foliar water uptake of Araucaria angustifolia. **Plant and Soil**, [*s.l.*], v. 399, n. 1–2, p. 147–157, 2016.

CASTELLI, M. et al. Two-source energy balance modeling of evapotranspiration in Alpine grasslandsRemote Sensing of Environment. **Remote Sensing of Environment**, [*s.l.*], v. 209, 2018.

CHEN, J. M.; LIU, J. Evolution of evapotranspiration models using thermal and shortwave remote sensing data. **Remote Sensing of Environment**, [*s.l.*], v. 237, p. 1–20, 2020.

COSGROVE, W. J.; LOUCKS, D. P. Water management: Current and future challenges and research directions. **Water Resources Research**, [*s.l*]., v. 51, n. 6, p. 4823–4839, 2015.

COSTA, C. A. G. et al. Spatial behaviour of soil moisture in the root zone of the Caatinga Comportamento espacial da umidade do solo na zona das raízes do Bioma Caatinga. **Revista Ciência Agronômica**, Fortaleza, v. 44, n. 4, p. 685–694, 2013.

COSTA, C. A. G. et al. Permanence of Water Effectiveness in the Root Zone of the Caatinga Biome. **Revista Caatinga**, Mossoró, v. 29, n. 3, p. 692–699, 2016.

COSTA, J. A. et al. Temporal dynamics of evapotranspiration in semiarid native forests in Brazil and Spain using remote sensing. **Hydrological Processes**, [*s.l.*], v. 35, p. 1–15, 2021.

DAHLEN, J.; SCHIMLECK, L.; SCHILLING, E. Modeling and Monitoring of Wood Moisture Content Using Time-Domain Reflectometry. **Forests**, [*s.l.*], v. 11, n. 479, 2020.

DE ALMEIDA, C. L.; DE CARVALHO, T. R. A.; DE ARAÚJO, J. C. Leaf area index of Caatinga biome and its relationship with hydrological and spectral variables. **Agricultural and Forest Meteorology**, [*s.l.*], v. 279, 2019.

DE ARAÚJO, J. C.; PIEDRA, J. I. G. Comparative hydrology: analysis of a semiarid and a humid tropical watershed. **Hydrological Processes**, [*s.l.*], v. 23, n. 8, p. 1169–1178, 2009.

DE FIGUEIREDO, J. V. et al. Runoff initiation in a preserved semiarid Caatinga small watershed, Northeastern Brazil. **Hydrological Processes**, [*s.l.*], v. 30, n. 13, p. 2390–2400, 2016.

DEL RÍO, S. et al. Analysis of recent trends in mean maximum and minimum temperatures in a region of the NW of Spain (Castilla y León). **Theoretical and Applied Climatology**, [*s.l.*], v. 90, p. 1–12, 2007.

DOMBROSKI, J. L. D. et al. Water relations of Caatinga trees in the dry season. **South African Journal of Botany**, [*s.l.*], v. 77, n. 2, p. 430–434, 2011.

DONATO, D. B. et al. Determinação da umidade da madeira em tora por diferentes métodos. **Pesquisa Florestal Brasileira**, Colombo, v. 34, n. 80, p. 449–453, 2014.

ELLER, C. B.; LIMA, A. L.; OLIVEIRA, R. S. Foliar uptake of fog water and transport belowground alleviates drought effects in the cloud forest tree species, Drimys brasiliensis (Winteraceae). **New Phytologist**, [*s.l.*], v. 199, n. 1, p. 151–162, 2013.

ELLER, C. B.; LIMA, A. L.; OLIVEIRA, R. S. Cloud forest trees with higher foliar water uptake capacity and anisohydric behavior are more vulnerable to drought and climate change. **The New phytologist**, [*s.l.*], v. 211, n. 2, p. 489–501, 2016.

FARIAS, T. R. L. et al. Unpaved rural roads as source areas of sediment in a watershed of the Brazilian semi-arid region. **International Journal of Sediment Research**, [*s.l.*], v. 34, n. 5, p. 475–485, 2019.

FERNÁNDEZ, V. et al. Wettability, Polarity, and Water Absorption of Holm Oak Leaves: Effect of Leaf Side and Age. **Plant Physiology Ò**, [*s.l.*], v. 166, p. 168–180, 2014.

FERREIRA, M. I. et al. Assessing hydraulic redistribution with the compensated average gradient heat-pulse method on rain-fed olive trees. **Plant and Soil**, [*s.l.*], v. 425, p. 21–41, 2018.

GATES, D. M. Transpiration and Leaf Temperature. **Annual Review of Plant Physiology**, [*s.l.*], v. 19, p. 211–238, 1968.

GOBBO, S. et al. Integrating SEBAL with in-Field Crop Water Status Measurement for Precision Irrigation Applications—A Case Study. **Remote Sensing**, [*s.l.*], v. 11, p. 1–18, 2019.

GOLDSMITH, G. R. Changing directions: The atmosphere-plant-soil continuum. **New Phytologist**, [*s.l.*], v. 199, n. 1, p. 4–6, 2013.

GOLDSMITH, G. R.; MATZKE, N. J.; DAWSON, T. E. The incidence and implications of clouds for cloud forest plant water relations. **Ecology Letters**, [*s.l.*], v. 16, n. 3, p. 307–314, 2013.

GOTSCH, S. G. et al. Foggy days and dry nights determine crown-level water balance in a seasonal tropical montane cloud forest. **Plant, Cell & Environment**, [*s.l.*], v. 37, n. 1, p. 261–272, 2014.

GROSSO, C. et al. Mapping Maize Evapotranspiration at Field Scale Using SEBAL: A Comparison with the FAO Method and Soil-Plant Model Simulations. **Remote Sensing**, [*s.l.*], v. 10, p. 1–17, 2018.

GÜNTNER, A.; BRONSTERT, A. Representation of landscape variability and lateral redistribution processes for large-scale hydrological modelling in semi-arid areas. **Journal of Hydrology**, [*s.l.*], v. 297, n. 1–4, 2004.

HAO, X. et al. Hydraulic lift in Populus euphratica Oliv. from the desert riparian vegetation of the Tarim River Basin. **Journal of Arid Environments**, [*s.l.*], v. 74, n. 8, p. 905–911, 2010.

HARTZELL, S.; BARTLETT, M. S.; PORPORATO, A. Plant Soil The role of plant water storage and hydraulic strategies in relation to soil moisture availability. **Plant and Soil**, [*s.l.*], v. 419, p. 503–521, 2017.

JAAFAR, H. H.; AHMAD, F. A. Time series trends of Landsat-based ET using automated calibration in METRIC and SEBAL: The Bekaa Valley, Lebanon. **Remote Sensing of Environment**, [*s.l.*], v. 238, p. 1–17, 2020.

KENDALL, M. G. **Rank Correlation Measures**. London: Charles Griffin, 1975.

KÖCHER, P.; HORNA, V.; LEUSCHNER, C. Stem water storage in five coexisting temperate broad-leaved tree species: significance, temporal dynamics and dependence on tree functional traits. **Tree Physiology**, [*s.l.*], v. 33, n. 8, p. 817–832, 2013.

KOOL, D. et al. A review of approaches for evapotranspiration partitioning. **Agricultural and Forest Meteorology**, [*s.l.*], v. 184, p. 56–70, 2014.

KOOL, D. et al. Energy and evapotranspiration partitioning in a desert vineyard. **Agricultural and Forest Meteorology**, [*s.l.*], v. 218, p. 277–287, 2016.

KROES, J. G. et al. **SWAP Version 3.2. Theory description and user manual**. 2. ed. Wageningen: Alterra, 2009.

LIANG, H. et al. Variation Characteristics of Stem Water Content in Lagerstroemia indica and Its Response to Environmental Factors. **Journal of Sensors**, [*s.l.*], v. 2020, p. 1-10, 2020.

LIAQAT, U. W.; CHOI, M. Surface energy fluxes in the Northeast Asia ecosystem: SEBS and METRIC models using Landsat satellite images. **Agricultural and Forest Meteorology**, [*s.l.*], v. 214–215, p. 60–79, 2015.

LIMA, A. L. A.; RODAL, M. J. N. Phenology and wood density of plants growing in the semi-arid region of northeastern Brazil. **Journal of Arid Environments**, [*s.l.*], v. 74, n. 11, p. 1363–1373, 2010.

LIMM, E. B. et al. Foliar water uptake: a common water acquisition strategy for plants of the redwood forest. **Oecologia**, [*s.l.*], v. 161, p. 449–459, 2009.

LITTELL, J. S. et al. A review of the relationships between drought and forest fire in the United States. **Global Change Biology**, [*s.l.*], v. 22, n. 7, p. 2353–2369, 2016.

LIU, C. et al. Environmental controls on seasonal ecosystem evapotranspiration/ potential evapotranspiration ratio as determined by the global eddy flux measurements. **Hydrology and Earth System Sciences**, [*s.l.*], v. 21, p. 311–322, 2017.

LOPES, J. R. G. et al. Reproductive losses caused by the ingestion of Poincianella pyramidalis in sheep. **Toxicon**, [*s.l.*], v. 138, p. 98–101, 2017.

LÓPEZ-BERNAL, Á.; TESTI, L.; VILLALOBOS, F. J. Using the compensated heat pulse method to monitor trends in stem water content in standing trees. **Tree Physiology**, [*s.l.*], v. 32, p. 1420–1429, 2012.

LOSGEDARAGH, S. Z.; RAHIMZADEGAN, M. Evaluation of SEBS, SEBAL, and METRIC models in estimation of the evaporation from the freshwater lakes (Case study: Amirkabir dam, Iran). **Journal of Hydrology**, [*s.l.*], v. 561, p. 523–531, 2018.

MANN, H. B. Nonparametric tests against trend. **Econometrica**, [*s.l.*], v. 13, p. 245–259, 1945.

MARENGO, J. A. et al. Assessing drought in the drylands of northeast Brazil under regional warming exceeding 4 °C. **Natural Hazards**, [*s.l.*], v. 103, p. 2589–2611, 2020.

MARSHALL, D. C. Measurement of sap flow in conifers by heat transport. **Plant Physiology**, [*s.l.*], v. 33, n. 6, p. 385–396, 1958.

MARTIN, C. E.; VON WILLERT, D. J. Leaf Epidermal Hydathodes and the Ecophysiological Consequences of Foliar Water Uptake in Species of Crassula from the

Namib Desert in Southern Africa. **Plant Biology**, [*s.l.*], v. 2, n. 2, p. 229–242, 2000.

MEDEIROS, P. H. A.; DE ARAÚJO, J. C. Temporal variability of rainfall in a semiarid environment in Brazil and its effect on sediment transport processes. **Journal of Soils and Sediments**, [*s.l.*], v. 14, n. 7, p. 1216–1223, 2014.

MEDEIROS, P. H. A.; DE ARAÚJO, J. C.; BRONSTERT, A. Interception measurements and assessment of Gash model performance for a tropical semi-arid region. **Revista Ciência Agronômica**, Fortaleza, v. 40, n. 2, p. 165–174, 2009.

MOLDEN, D. et al. Improving agricultural water productivity: Between optimism and caution. **Agricultural Water Management**, [*s.l.*], v. 97, n. 4, p. 528–535, 2010.

MORATIEL, R. et al. Natural Hazards and Earth System Sciences Trends in climatic variables and future reference evapotranspiration in Duero Valley (Spain). **Hazards Earth Syst. Sci**, [*s.l.*], v. 11, p. 1795–1805, 2011.

MORENO-FERNÁNDEZ, D. et al. Regeneration dynamics of mixed stands of Pinus pinaster Ait. and Pinus pinea L. in Central Spain. **Eur J Forest Res**, [*s.l.*], v. 137, p. 17–27, 2018.

NADEZHDINA, N. et al. Trees never rest: the multiple facets of hydraulic redistribution. **Ecohydrology**, [*s.l.*], v. 3, n. 4, p. 431–444, 2010.

NOBEL, P. S. **Physico chemical and environmental plant physiology**. 4. ed. Oxford: Academic Press, 2009.

OLIVEIRA, R. S. et al. The hydroclimatic and ecophysiological basis of cloud forest distributions under current and projected climates. **Annals of Botany**, [*s.l.*], v. 113, p. 909–920, 2014.

PENNA, D. et al. Soil moisture temporal stability at different depths on two alpine hillslopes during wet and dry periods. **Journal of Hydrology**, [*s.l.*], v. 477, p. 55–71, 2013.

PINA, A. L. C. B. et al. Dew absorption by the leaf trichomes of Combretum leprosum in the Brazilian semiarid region. **Functional Plant Biology**, [*s.l.*], v. 43, n. 9, p. 851–861, 2016.

PINHEIRO, E. A. R. et al. Importance of soil-water to the Caatinga biome, Brazil. **Ecohydrology**, [*s.l.*], v. 9, n. 7, p. 1313–1327, 2016.

PINHEIRO, E. A. R.; VAN LIER, Q. DE J.; METSELAAR, K. A Matric Flux Potential Approach to Assess Plant Water Availability in Two Climate Zones in Brazil. **Vadose Zone Journal**, [*s.l.*], v. 15, p. 1–10, 2018.

RAHIMZADEGAN, M.; JANANI, A. S. Estimating evapotranspiration of pistachio crop based on SEBAL algorithm using Landsat 8 satellite imagery. **Agricultural Water Management**, [*s.l.*], v. 217, p. 383–390, 2019.

SAFRIEL, U.; ADEEL, Z. Dryland Systems. In: HASSAN, R.; SCHOLES, R.; ASH, N. (Eds.). . **Ecosystems and human well-being, current state and trends**. 1. ed. Washington: Island Press, 2005.

SANTOS, J. C. N. DOS et al. Land use impact on soil erosion at different scales in the Brazilian semi-arid. **Revista Ciência Agronômica**, Fortaleza, v. 48, n. 2, p. 251–260, 2017.

SCHUMACHER, F. X.; HALL, F. DOS S. LOGARITHMIC EXPRESSION OF TIMBER-TREE VOLUME. **Journal of Agricultural Research**, [*s.l.*], v. 47, n. 9, 1933.

SENKONDO, W. et al. Comparing remotely-sensed surface energy balance evapotranspiration estimates in heterogeneous and data-limited regions: A case study of Tanzania's Kilombero Valley. **Remote Sensing**, [*s.l.*], v. 11, p. 1–33, 2019.

SIMONIN, K. A.; SANTIAGO, L. S.; DAWSON, T. E. Fog interception by Sequoia sempervirens (D. Don) crowns decouples physiology from soil water deficit. **Plant, Cell and Environment**, [*s.l.*], v. 32, n. 7, p. 882–892, 2009.

SIMPLÍCIO, A. A. F. et al. Erosion at hillslope and micro-basin scales in the Gilbués desertification region, Northeastern Brazil. **Land Degradation & Development**, [*s.l.*], v. 32, n. 3, p. 1487–1499, 2021.

SUN, H. et al. Improving estimation of cropland evapotranspiration by the Bayesian model averaging method with surface energy balance models. **Atmosphere**, [*s.l.*], v. 10, p. 1–19, 2019.

TASUMI, M. Estimating evapotranspiration using METRIC model and Landsat data for better understandings of regional hydrology in the western Urmia Lake Basin. **Agricultural Water Management**, [*s.l.*], v. 226, p. 1–11, 2019.

TEIXEIRA, A. H. DE C. et al. Reviewing SEBAL input parameters for assessing evapotranspiration and water productivity for the Low-Middle Sã o Francisco River basin, Brazil Part A: Calibration and validation. **Agricultural and Forest Meteorology**, [*s.l.*], v. 149, p. 462–476, 2009.

TEIXEIRA, L. M. N. **Evapotranspiração em vegetação natural do bioma Caatinga obtida por balanço hídrico no solo e por sensoriamento remoto**. 2018. 121 f. Thesis (Mestrado em Engenharia Agrícola)-Universidade Federal do Ceará, Fortaleza, 2018.

TILESSE, F. E. A. DE et al. Stem water storage potential in plants of the Caatinga biome. **Ciência Agronômica**, Fortaleza, v. 52, n. 3, 2021.

TYREE, M. T.; ZIMMERMANN, M. H. **Xylem Structure and the Ascent of Sap**. 2. ed. New York: Springer, 2002.

VÁSQUEZ-MÉNDEZ, R. et al. Soil erosion and runoff in different vegetation patches from semiarid Central Mexico. 2009.

VERGARECHEA, M. et al. Climate-mediated regeneration occurrence in Mediterranean pine forests: A modeling approach. **Forest Ecology and Management journal**, [*s.l.*], v. 446, p. 10–19, 2019.

VICENTE-SERRANO, S. M. et al. Reference evapotranspiration variability and trends in Spain, 1961-2011. **Global and Planetary Change**, [*s.l.*], v. 121, p. 26–40, 2014.

WANG, X. et al. Canopy storage capacity of xerophytic shrubs in Northwestern China. **Journal of Hydrology**, [*s.l.*], v. 454–455, p. 152–159, 2012.

WILCOX, B. P.; BRESHEARS, D. D.; SEYFRIED, M. S. Water Balance on Rangelands. **Encyclopedia of Water Science**, New York, p. 791–794, 2003.

WRIGHT, C. L. et al. Plant functional types broadly describe water use strategies in the Caatinga, a seasonally dry tropical forest in northeast Brazil. **Ecology and Evolution**, [*s.l.*], v. 11, n. 17, p. 11808–11825, 2021.

YANG, Z. et al. Changes in evapotranspiration over global semiarid regions 1984–2013. **Journal of Geophysical Research: Atmospheres**, [*s.l.*], v. 124, p. 1–18, 2019.

YU, T. et al. Hydraulic redistribution of soil water by roots of two desert riparian phreatophytes in northwest China's extremely arid region. **Plant and Soil**, [*s.l.*], v. 372, n. 1–2, p. 297–308, 2013.

ZHAO, M. et al. Soil water dynamics based on a contrastive experiment between vegetated and non-vegetated sites in a semiarid region in Northwest China. **Journal of Hydrology**, [*s.l.*], v. 603, p. 126880, 2021.

ZHAO, Y. et al. Controls of surface soil moisture spatial patterns and their temporal stability in a semi-arid steppe. **Hydrological Processes**, [*s.l.*], v. 24, n. 18, p. 2507–2519, 2010.